Department of Veterans Affairs

Journal of Rehabilitation Research and Development Vol. 34 No. 1, January 1997
Pages 19–43

Interface pressures and shear stresses at thirteen socket sites on two persons with transtibial amputation

Joan E. Sanders, PhD; Dickson Lam; Alan J. Dralle, CP; Ramona Okumura, CP
Center for Bioengineering and Department of Rehabilitation Medicine, University of Washington, Seattle, WA 98195

Abstract—Residual limb/prosthetic socket interface pressures and shear stresses were measured at 13 sites on two subjects with unilateral transtibial amputation (TTA) using total-contact patellar-tendon-bearing prostheses. Maximal interface stresses during stance phase for each of 13 transducer sites were determined, then means for all steps calculated. Maximal pressure and resultant shear stress during stance phase were shown at anterior distal or mid-limb sites and the maxima occurred during the first 50% of stance phase. Anterior medial and lateral proximal sites showed their greatest pressure during the second 50%. At lateral mid-limb and popliteal fossa sites, resultant shear stress directions suggest that soft tissue was displaced toward the socket brim during weight-bearing. Results also suggest that skin across the distal tibial crest was in tension at the times of the first and second peaks in the shank axial force-time curve in all sessions. Significant differences ($p<0.05$) in maximal stresses between sessions conducted >3 weeks apart were apparent for both subjects.

Key words: *interface mechanics, interface pressures, interface stress, lower-limb prosthetics, shear stress, transtibial amputation.*

INTRODUCTION

Interface stresses are an important consideration in fitting a prosthetic limb to a person with lower-limb amputation. Because soft tissues of the thigh and lower leg are not accustomed to bearing the interface pressures and shear stresses induced by a prosthesis, the tissues are susceptible to pain, discomfort, and breakdown. Once tissue breakdown occurs, typically a period of reduced activity is required. In severe cases, no prosthesis use is possible, and surgical repair or modification of the residual limb is necessary. To avoid breakdown, prostheses must be designed so that sensitive tissue regions receive lower absolute magnitude stresses; more tolerant regions can receive higher stresses. An important aspect of fitting is to design a prosthesis that induces an interface pressure and shear stress distribution acceptable for tissue tolerance.

Several studies investigating interface stress distributions on persons with lower limb amputation during walking are described in the literature (1–15). The identification of patterns in the pressures and shear stresses that occur has been of particular interest. For example, Appoldt searched for ranges of interface "tangential pressures" (a term all-inclusive for stresses tangent to the interface, whether or not slip occurred) deemed significant to the comfort and employment of above-knee suction sockets on persons with transfemoral amputation (3). The utility of those data is to further understand the magnitudes of stresses residual limb soft tissues must tolerate, identify trends in interface loading applicable to prosthetic design in a general sense, and provide a base for comparison with stresses produced by prosthesis modifications. Interface stress data are also used for evaluation of residual limb/socket finite element (FE) models (16–19), computer-based analysis tools that calculate interface stresses based on residual limb and prosthesis geometries and material properties as well as the loading conditions specified at the model boundaries (e.g., ground reaction forces on the prosthesis during weight-bearing). FE models have been used principally for inter-

This material is based upon work supported by the National Institute of Child and Human Development.
Address all correspondence and requests for reprints to: Joan E. Sanders, PhD, Assistant Professor, Center for Bioengineering, Box 357962, University of Washington, Seattle, WA 98195; email: sanders@limbs.bioeng.washington.edu.

face stress sensitivity analysis to residual limb and prosthesis characteristics (17,19–23).

The purpose of this research was to expand upon previous interface stress studies to measure interface pressures and shear stresses at more sites, 13, than previously reported on subjects with transtibial amputation (TTA) walking with total contact patellar-tendon-bearing (PTB) prostheses. Consistency of the results with findings reported in the literature was evaluated, and new issues concerning interface stress mechanics were addressed. Five features were investigated for stance phase on the prosthetic limb for all steps in each session:

1. Interface stress magnitudes for each transducer site: (i) maximal stance phase pressure for the site, (ii) maximal stance phase resultant shear stress (RS) and the corresponding resultant shear angle (RSang) for the site, (iii) pressure and RS at the time of the first peak in the shank axial force-time curve (1st pk), and (iv) pressure and RS at the time of the second peak in the shank axial force-time curve (2nd pk);
2. Timings of the stance phase pressure and RS maxima for each site;
3. RSang for each site during the time interval between the 1st pk and 2nd pk (approximately mid-stance phase);
4. Waveform shape similarities and differences among different sites;
5. Temporal (session-to-session) changes in pressure and RS maxima at each site.

Throughout this article, a consistent reference frame is used for discussion of interface stress directions. Stresses applied to the transducers are presented as opposed to stresses applied to the residual limb. In this study, transducers were mounted in the socket wall. When there is no slip at the residual limb/prosthetic socket interface, stresses applied to the transducers (socket) are equal in magnitude but opposite in direction to those applied to the residual limb. When there is slip at the interface, transducers measure the frictional stress between the residual limb and prosthetic socket.

METHODS

Subjects

Two male subjects, TW and WP, with unilateral TTA participated in this research. Both had amputations at least 2 years prior to the study, having suffered traumatic injuries (motor vehicle accidents) and had been receiving prosthetic care from the University of Washington

Table 1.
Subject and prosthesis information.

Parameter	Subject TW	Subject WP
sex	male	male
age	31 years	47 years
mass	65.9 kg	72.7 kg
height	173 cm	180 cm
time since amputation	20 years	21 years
residual limb	right	left
residual limb length (mid-patellar-tendon to distal tibia)	20.3 cm	14.0 cm
residual limb diameter (at tibial condyles)	9.2 cm	9.8 cm
prosthetic limb length (mid-patellar tendon to bottom of foot)	44.5 cm	47.6 cm
inside socket circumference at ALP/AMP sites	30.7 cm	33.8 cm
inside socket circumference at ALM/AMM sites	25.0 cm	33.0 cm
inside socket circumference at ALD/AMD sites	23.5 cm	31.5 cm
qualitative description of residual limb	long residual limb with relatively little soft tissue throughout the length.	mature residual limb with some scarring on the distal end
clinical comments	for his regular prosthesis he needed to use a supracondylar strap to limit his knee extension range; usually used a FlexFoot	had quite a bit of lateral thrust at the knee during stance; usually used a Seattle or SACH foot

ALP = anterior lateral proximal; AMP = anterior medial proximal; ALM= anterior lateral mid-limb; AMM = anterior medial mid-limb; ALD = anterior lateral distal; AMD = anterior medial distal.

Department of Rehabilitation Medicine for at least 2 years.

The residual limbs of the two subjects had strongly contrasting biomechanical features (**Table 1**). TW had a longer residual limb than WP and much less soft tissue through the length. In addition, componentry of the normal prostheses of the subjects were different: TW usually wore a suprapatellar strap and used a FlexFoot™, while WP did not wear a strap and usually used a Seattle™ or SACH foot.

Instrumented Prosthesis

Prosthetic sockets used in the research were designed and fabricated by a certified prosthetist (for WP) and by a student prosthetist under the supervision of a certified prosthetist (for TW). The sockets were made and fit to the subjects approximately 10 months before the data reported here were collected for WP and 4 months before for TW. The sockets were of PTB design and were standard PTB laminated polyester approximately 4 mm thick, designed and manufactured using traditional (as opposed to computer-aided) techniques. They were total contact sockets of laminated acrylic resin using perlon and a nylon stockinet under vacuum and made from a plaster negative, hand modified, and test-socket fitted. Static and dynamic alignment were conducted using standard clinical techniques (24) until the fit was deemed acceptable by the subjects and certified prosthetists. (Note that dynamic alignment was repeated after the prosthesis was instrumented.) The test prostheses were not used regularly by the subjects.

Sockets were instrumented with mounts bonded to the outside to hold interface stress transducers (**Figure 1**). Interface stress transducers and signal conditioning circuitry have been described in detail elsewhere (25,26). For the 13 transducer/signal conditioning units used in this study, transducer RMS measurement errors (nonlinearity determined from calibration test data) averaged 3.90 ± 1.57 percent of the full-scale output (FSO) for the normal direction (pressure) and 0.22 ± 0.29 percent FSO for the shear directions (horizontal and vertical shear stress). Reference marks on the transducers, made during calibration testing, identified the stress directions. In this article, the term "pressure" is used rather than "normal stress" to describe the force/surface area measurement in the direction normal to the transducer surface. As in previous investigations (12,15), it is assumed stresses are uniformly distributed over the sensor surface.

Polycarbonate mounts (mass 4.7 g each, internally threaded with 32 threads per in—12.6 per cm) were positioned in 12.7 mm diameter holes through the socket wall, affixed to the socket using epoxy (DP-460, Scotch-Weld, 3M, St. Paul, MN), and aligned using a custom tool that set their central axes perpendicular to the inner surface. Care was taken to position mounts only at relatively flat sites on the socket to minimize modification to the original socket shape. Where the hole on the socket surface was not in one plane, epoxy was used on the inside socket surface to smooth the edge between the mount and the surrounding interface (**Figure 1**). Thus, the inside socket surface remained free of sharp edges. The epoxy layer was thicker at posterior sites than at anterior or lateral sites, though it was typically less than 1 mm.

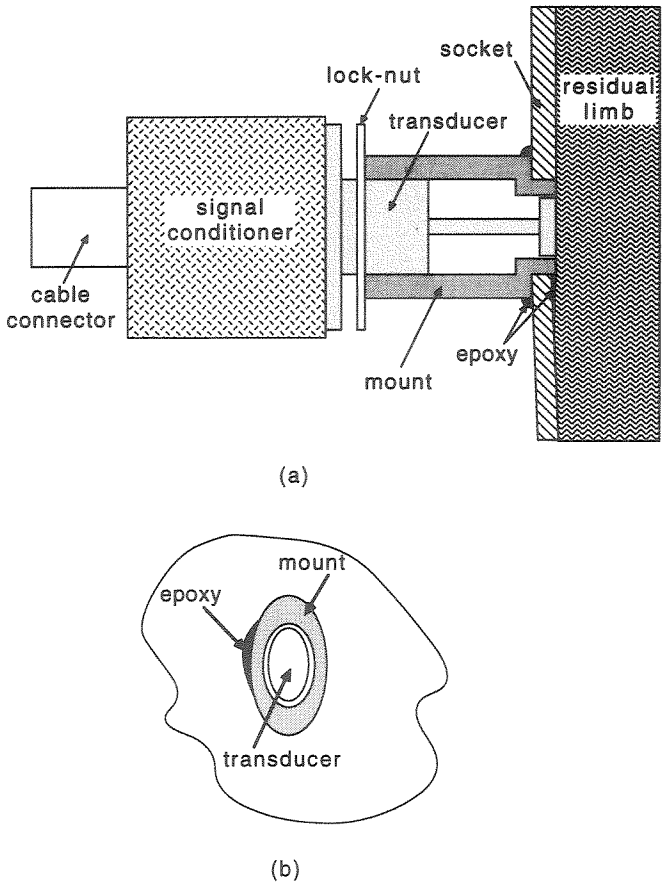

Figure 1.
a. Side view of a transducer in a mount. The transducer was positioned flush with the interface. b. A transducer and mount viewed from inside the socket. Epoxy was used to smooth the mount edge with the surrounding surface.

Transducers were positioned in the mounts with their surfaces flush with the inner mount face, using another custom tool that covered the face of the mount inside the socket. A transducer was advanced into the mount until it contacted the tool, a technique that resulted in a repeatable transducer position within 10° of transducer rotation in the mount. At the thread pitch used (12.6 threads per cm), the 10° error corresponded to 0.02 mm of axial translation, far less than the 1.6 mm of transducer protrusion evaluated by Appoldt (27), shown to have an effect on interface stress measurements. For each subject, the same transducers were used at the same sites at the same axial positions in different sessions.

All sites were carefully checked to ensure that the 6.35 mm diameter transducer did not contact the 7.60 mm hole in the mount during full-scale shear loading. So that transducer principal shear directions with respect to the shank axis could later be identified, reference marks were made on the top outer edge of each mount. The prosthesis was mounted in a dividing head on a milling machine and a scribe tool placed in the collet to make the reference marks, to ensure that marks were at the most proximal location for each mount. The angles of the transducer principal shear axes with respect to the mount were recorded using an angle scale between reference marks on the transducers and those on the mounts. Measurements of the transducer principal shear directions were accurate to within 2° of transducer rotation, which corresponded to 0.004 mm of axial translation of the transducer in the mount. These measurements were used to transform the shear stress data into referenced coordinate systems. "Vertical shear stress" was in the plane of the interface in a direction longitudinal with respect to the socket axis. "Horizontal shear stress" was in the plane of the interface in a direction transverse to the socket axis. A neoprene sleeve was used for suspension by both subjects.

A total of 13 interface sites was monitored, the maximal number that could reasonably fit on each socket without adjacent transducers contacting (**Figure 2**). None were positioned on the medial surface, since they would have interfered with the contralateral limb. Transducers were positioned in three regions (groups): anterior, lateral, and posterior (**Table 2**). It is important to note that the locations described in **Table 2** and in the text below refer to the residual limb as opposed to the socket, as anatomical landmarks are appropriately descriptive for this purpose. The transducer locations on the socket correspond to these landmarks, assuming the residual limb is well in

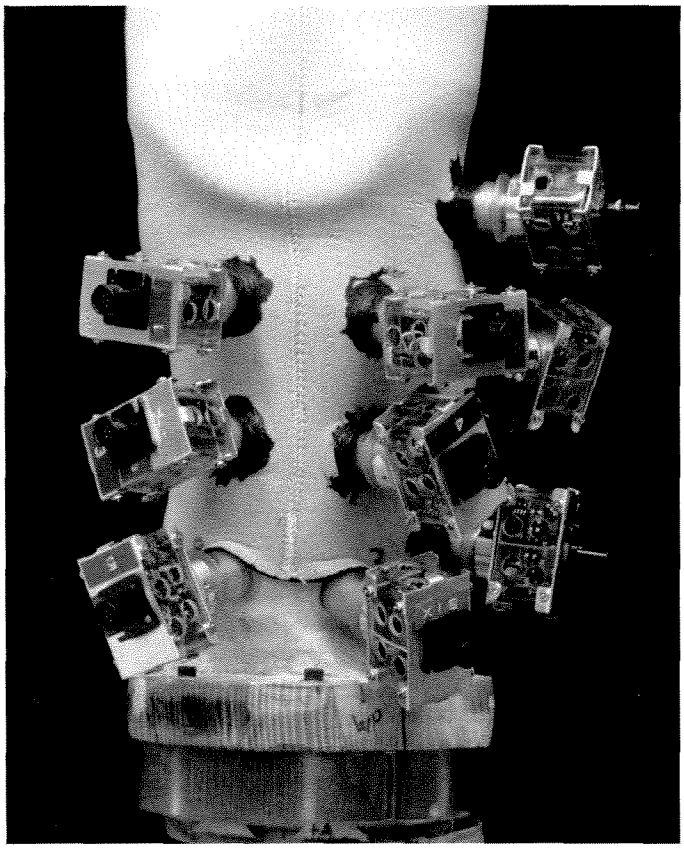

Figure 2.
A test socket instrumented with 13 transducers is shown. Each box contains signal-conditioning instrumentation for the three channels from the transducer. Cables from signal conditioners to the waist belt pack are not shown.

the socket as achieved during weight-bearing. Transducers were in similar locations for both subjects. Six were on the anterior surface (ALD, AMD, ALM, AMM, ALP, AMP), three on each side of the anterior surface longitudinal midline. Two were at the transverse level of the tibial tubercle (ALP, AMP), two were at the most distal level on the tibial flare (ALD, AMD), and two (the mid-limb pair: ALM, AMM) were halfway between the tibial tubercle and distal pairs. Anterior surface transducers were positioned close to the socket relief for the tibial crest, hereafter referred to as the "anterior apex" region of the socket, but still on relatively flat surfaces that contacted the tibial flares. Transducers on the posterior surface (PD, PM, PF) were all along the posterior longitudinal midline. The most proximal (PF) was at the maximal indentation at the popliteal fossa. PM was at the transverse level of the AMM transducers. PD was approximately 2 cm proximal of the transverse level of the ALD

Table 2.
Transducer locations.

Group	Site Abbreviation	Site Name	Transducer Location
Anterior Group	ALD	anterior lateral distal	distal residual limb, anterior tibial border, lateral side
	AMD	anterior medial distal	distal residual limb, anterior tibial border, medial side
	ALM	anterior lateral mid-limb	mid, anterior tibial border, lateral side
	AMM	anterior medial mid-limb	mid, anterior tibial border, medial side
	ALP	anterior lateral proximal	at the level of the tibial tubercle, lateral side
	AMP	anterior medial proximal	at the level of the tibial tubercle, medial side
Lateral Group	LD	lateral distal	lateral distal residual limb
	LPD	lateral-posterior distal	midway between the lateral distal fibula and distal calf (on the border between the lateral and posterior groups)
	LM	lateral mid-limb	fibular neck
	LP	lateral proximal	lateral femoral epicondyle
Posterior Group	PD	posterior distal	distal calf, on the posterior longitudinal midline
	PM	posterior mid-limb	mid-calf, on the posterior longitudinal midline
	PF	popliteal fossa	center of the popliteal fossa, on the posterior longitudinal midline

and AMD transducers. It was positioned here because in preliminary studies it was found that subjects typically did not bear load on the posterior surface at the transverse level of the anterior distal (AD) transducers. For the lateral group (LD, LPD, LM, LP), LP was in the region of the lateral femoral condyle, on a line between the anterior proximal (AP) and PF transducers and on a socket midline through the sagittal plane. LD was at the level of a transverse plane halfway between the PD and PM sites, also on a socket midline through the sagittal plane. The LPD site was at the border between the lateral and posterior groups, at the level of a transverse plane between the LD and PM sites. It was not on a socket midline in the sagittal plane but instead on the socket surface halfway between the sagittal plane socket midline and the posterior midline. The LM transducer was in the fibular neck region but was positioned at different sites for the two subjects, 2.0 cm distal to the fibular head on TW and 2.5 cm posterior of the fibula at the transverse level of the fibular head on WP to avoid contact between adjacent transducers. It should be noted that holes were made in the neoprene sleeves to allow several transducers to be positioned more proximally than described in previous reports from our laboratory on other subjects (12,15).

In data collection sessions, each subject wore a 5-ply wool sock but no liner between the socket and the residual limb. Thus, the transducers measured socket-sock interface stresses, not stresses directly on the skin surface. Previously, Pelite™ was mounted on the end of each transducer and Pelite liners, but no socks, were worn by subjects (12,15). The basis for changing to the new configuration was a clinical concern. Donning a prosthesis without a sock but with a liner bonded to its inside surface was uncomfortable for the subjects and deemed an unacceptable tissue health risk here.

The prosthetic shank was also instrumented. Forces and moments in the shank were measured using 20 strain-gages mounted on an aluminum pylon, and the data used to identify heel contact and toe-off as well as timings of 1st and 2nd pks. The instrumented shank was a slight modification of that described previously (28). Custom-designed tight-fit aluminum inserts epoxied in the ends of the pylon (necessary to ensure uniform hoop stress) were more lightweight, and a Proteor™ alignment jig (Durr-Fillauer, Chattanooga, TN) was used to attach the shank to the prosthesis. A Seattle LightFoot™ (size and stiff-

ness established by the prosthetist and subject) was connected to the shank.

From the instrumented socket and shank, cables ran to a belt pack for multiplexing the 45 channels of data (39 channels from the transducers, 6 from the shank) onto 3 channels. A 58 m shielded cable carried the data from the belt pack to an A/D board and computer for acquisition and storage (NB-MIO-16, National Instruments, Austin, TX; 650 Centris, Apple Computer, Cupertino, CA). Data were collected at a 175 Hz sampling rate, a rate determined appropriate from data analysis in previous investigations if high-frequency events in interface stress-time curves are of interest (15). The mass of the instrumented prosthesis was 2.32 kg, 0.41 kg of which was the transducers and 0.36 kg of which was the pylon with insert connectors. The mass of the belt pack was 1.46 kg.

The instrumented prostheses were aligned using standard clinical static and dynamic fitting techniques (24). After the "neutral" alignment was set by the prosthetists, at least one preliminary session was conducted to allow the subject to become accustomed to the instrumentation, to make minor adjustments that the prosthetists deemed necessary, and to evaluate performance of the instrumentation. Data from preliminary sessions are not included in the results. WP had three preliminary sessions during the 3-month period before the start of the study, and TW had one, approximately 1 month before the start of the study.

During their three or more trials, subjects walked up and down a 68 × 2.1 m hallway at a self-selected speed. The data acquisition system was in a recess midway down the hall, thus the cable length was not restrictive. Data were collected for 20 s in each trial, during which time the subject, starting from a standstill, walked the length of the hallway between three-quarters to one and one-half times.

Post-processing was conducted to transform the data into a socket-referenced coordinate system (as shown in **Figure 3** and described below). Steps were then segmented into stance and swing phase, based on a threshold slope in the shank pylon axial force-time waveform. As in previous studies (12), the threshold was 0.63 N/msec for heel-contact and −0.63 N/msec for toe-off. Steps at a much slower speed than those of the rest of the trial (e.g., while the subject turned around at the end of the hallway) were not included. Only the stance phase of gait was analyzed further. The following information was determined for each step: maximal magnitudes of interface pressure and RS (and the corresponding RSang) at each transducer site and the percentage of stance phase that they occurred; interface pressures, RS, and RSang for all sites at the times of the 1st pk and 2nd pk in the shank axial force-time curves. T-tests at a level 0.05 (p-value) test were used to compare differences between sites and sessions discussed below. In addition, a custom computer program (using Matlab, MathWorks, Inc., Natick, MA) was written to display stance phase interface stress-time curves from multiple steps and multiple sites simultaneously (sites and steps selected by the user) as well as polar plots (r-θ) of RS (r) and RSang (θ), allowing visual inspection for similarities and differences in interface stress-time curve shapes.

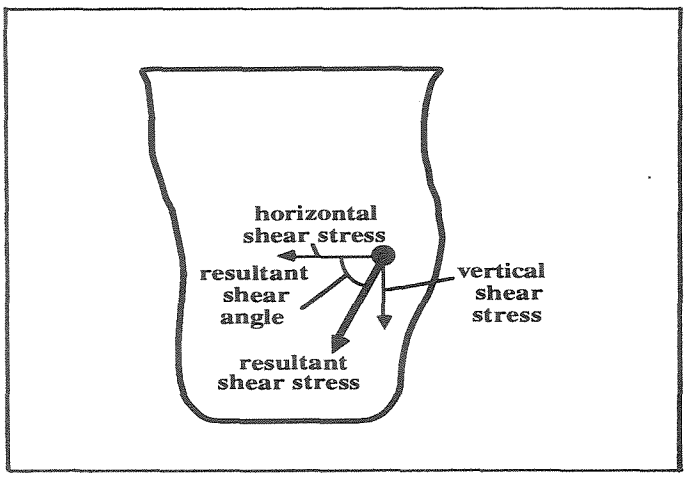

Figure 3.
The coordinate system convention used throughout for shear stress. Shear stresses applied to the socket (as shown here) are positive in sign. Shear stresses are in the plane of the interface with the RSang defined counter-clockwise relative to the horizontal shear positive axis. An anterior lateral mid-limb site is shown.

RESULTS

Interface stress data are presented such that stresses on the transducers (on the socket) are positive in sign. "Shear stress" is the force measured by the transducer, whether or not slip occurs, divided by its surface area. A positive horizontal shear stress is clockwise when viewing the socket from above. Vertical shear stress is positive when directed distally. A pressure (normal stress) applied from the residual limb toward the socket is positive in sign. For the results presented below, typically RS and RSang are presented rather than horizontal and vertical shear stresses. RSs are the resultant of the horizontal and

vertical shear components, and the RSang is relative to the horizontal shear axis (**Figure 3**). Only data from the stance phase of gait are presented below. Swing phase interface stresses were less than maximal stance phase stresses at all sites on both subjects.

Two sessions were conducted on each subject, 21 days apart for TW and 42 days apart for WP. They all were conducted during morning hours: session TW812 started at 10:04 a.m.; TW92 at 10:32 a.m.; WP1024 at 10:21 a.m.; and WP125 at 9:20 a.m. After the TW92 data were collected, the subject complained that he felt that he had been "bottoming out" (residual limb contacted the distal end of the socket in stance phase) during the walking trials. As no powder transfer test between the residual limb and the bottom of the socket was conducted, only the verbal description from the subject is available. The prosthetists noted that WP's residual limb underwent shrinkage after the socket was fabricated. For both subjects, the prosthetists considered the fit sub-optimal but acceptable for short-term ambulation.

At least 23 steps on the prosthesis were collected at neutral alignment in each session. Stance phase durations were 0.69±0.03 s for TW812, 0.72±0.05 s for TW92, 0.90±0.04 s for WP1024, and 0.87±0.08 s for WP125. Stance phase durations as a percentage of step durations were 61.36±0.99 percent for TW812, 61.53±1.84 percent for TW92, 63.12±1.04 percent for WP1024, and 63.96±1.16 percent for WP125.

Some of the channels did not function properly in some of the sessions. They are shown as nonfunctional (NF) in **Tables 3–6**. NF channels were always the result of a broken wire connection in the transducer or signal-conditioning box. Findings below are based on cases where transducers functioned and comparisons could be made.

Pressure and Resultant Shear Stress Maxima

Maximal interface pressures and RSs during stance phase for all transducers were determined for each step and the means and standard deviations (SD) for all steps at each site in each session computed. Maximal stresses are considered in analysis because they are potentially the most traumatic to the tissues.

For all sessions, an anterior site always had the highest mean maximal pressure and mean maximal RS, as shown in **Tables 3a, 3c**, and **3e**. The LP site showed the lowest pressure maxima during stance phase in all sessions but not always the lowest RS maxima.

Significant (significance in all cases: $p<0.05$) stress differences were apparent for transducers within each group (anterior, lateral, posterior) and between groups. For both pressure and RS for both subjects, maximal stresses were significantly greater at either AD transducer site compared with either AP site, as shown in **Table 3a**. AMD pressure maxima were significantly higher than ALD pressure maxima in three of the four sessions. PM pressure maxima were significantly greater than PD pressure maxima, and RS maxima were significantly higher at PD sites than at PM locations (**Table 3e**). Pressure maxima at the PF site were significantly greater than

Table 3a.
Peak interface stresses during stance phase: anterior region magnitudes.

Session	Parameter	ALD	AMD	ALM	AMM	ALP	AMP
TW812	PR	142.5 ± 12.5	140.0 ± 3.4	103.2 ± 4.5	85.5 ± 6.5	17.6 ± 6.3	14.1 ± 2.3
	RS	60.1 ± 4.1	43.3 ± 2.8	11.5 ± 1.2	11.9 ± 1.8	2.4 ± 0.5	1.6 ± 0.2
	RSang (θ)	111.7 ± 1.4	92.3 ± 3.3	155.4 ± 19.5	87.6 ± 49.4	234.6 ± 9.1	28.8 ± 24.8
TW92	PR	212.3 ± 18.5	223.8 ± 30.0	99.5 ± 10.0	87.3 ± 14.3	NF	29.2 ± 4.0
	RS	48.8 ± 5.3	48.3 ± 13.4	9.2 ± 1.6	7.1 ± 2.2	NF	2.6 ± 0.5
	RSang (θ)	99.0 ± 2.4	94.4 ± 4.5	211.1 ± 16.8	314.8 ± 68.5	NF	37.6 ± 16.8
WP1024	PR	99.3 ± 8.4	145.1 ± 46.4	107.8 ± 0.1	157.7 ± 38.9	NF	NF
	RS	24.4 ± 2.8	66.1 ± 10.1	23.5 ± 2.5	7.4 ± 1.5	NF	NF
	RSang (θ)	17.6 ± 3.8	104.6 ± 7.2	73.5 ± 10.5	150.8 ± 10.6	NF	NF
WP125	PR	103.0 ± 8.4	132.5 ± 25.2	52.2 ± 3.0	155.7 ± 18.9	40.6 ± 10.2	54.0 ± 5.9
	RS	20.8 ± 2.0	30.0 ± 4.6	28.3 ± 2.2	16.2 ± 3.8	3.6 ± 0.5	8.5 ± 0.8
	RSang (θ)	86.3 ± 16.4	143.8 ± 6.2	104.3 ± 2.8	64.1 ± 10.1	13.8 ± 42.0	190.1 ± 6.0

Magnitudes are expressed in kPa, angles in degrees; means ± SD for all steps in each session are shown. ALD = anterior lateral distal; AMD = anterior medial distal; ALM = anterior lateral mid-limb; AMM = anterior medial mid-limb; ALP = anterior lateral proximal; AMP = anterior medial proximal; PR = pressure; RS = resultant shear stress; RSang (θ) = resultant shear angle at the time of peak RS; NF = nonfunctional transducer.

Table 3b.
Peak interface stresses during stance phase: anterior region timings.

Session	Parameter	ALD	AMD	ALM	AMM	ALP	AMP
TW812	PR	26.4 ± 13.0	27.4 ± 5.1	31.1 ± 19.6	25.9 ± 1.3	91.1 ± 0.8	86.1 ± 16.1
	RS	23.0 ± 2.6	26.5 ± 3.0	64.2 ± 28.1	23.6 ± 7.4	91.3 ± 1.2	84.4 ± 14.5
TW92	PR	25.2 ± 2.1	26.0 ± 2.3	26.3 ± 10.1	25.0 ± 2.4	NF	85.8 ± 3.8
	RS	23.9 ± 3.6	25.8 ± 15.1	24.3 ± 18.8	28.5 ± 24.8	NF	71.0 ± 24.9
WP1024	PR	34.1 ± 3.3	35.0 ± 23.5	50.3 ± 22.6	32.6 ± 2.5	NF	NF
	RS	34.4 ± 2.7	48.5 ± 36.7	75.2 ± 24.3	23.5 ± 13.7	NF	NF
WP125	PR	36.0 ± 7.9	27.1 ± 5.2	42.1 ± 10.6	30.8 ± 8.4	74.4 ± 7.8	75.4 ± 9.3
	RS	44.2 ± 13.9	29.1 ± 4.5	64.4 ± 16.2	38.3 ± 7.4	41.3 ± 16.6	42.5 ± 6.8

Timings are expressed in percentage of stance phase; means ± SD for all steps in each session are shown. ALD = anterior lateral distal; AMD = anterior medial distal; ALM = anterior lateral mid-limb; AMM = anterior medial mid-limb; ALP = anterior lateral proximal; AMP = anterior medial proximal; PR = pressure; RS = resultant shear stress; RSang (θ) = resultant shear angle at the time of peak RS; NF = nonfunctional transducer.

Table 3c.
Peak interface stresses during stance phase: lateral region magnitudes.

Session	Parameter	LD	LPD	LM	LP
TW812	PR	79.8 ± 0.1	NF	63.6 ± 5.8	9.6 ± 0.9
	RS	17.7 ± 1.2	NF	9.8 ± 0.8	3.5 ± 0.2
	RSang (θ)	140.9 ± 4.3	NF	204.9 ± 5.4	289.8 ± 11.9
TW92	PR	180.7 ± 18.6	90.0 ± 14.4	64.1 ± 5.0	16.8 ± 1.9
	RS	4.3 ± 0.6	5.6 ± 0.9	8.3 ± 0.8	2.5 ± 0.4
	RSang (θ)	105.9 ± 8.9	73.1 ± 5.8	215.6 ± 4.7	272.0 ± 76.3
WP1024	PR	87.0 ± 5.4	77.9 ± 3.7	54.6 ± 5.3	28.3 ± 9.2
	RS	6.4 ± 1.8	1.5 ± 0.2	8.2 ± 0.3	5.4 ± 1.5
	RSang (θ)	81.4 ± 11.0	44.7 ± 83.6	265.9 ± 1.4	117.2 ± 7.9
WP125	PR	97.7 ± 4.6	87.0 ± 6.8	62.7 ± 6.7	18.2 ± 6.4
	RS	5.7 ± 1.1	6.2 ± 1.1	5.0 ± 0.5	3.2 ± 0.6
	RSang (θ)	95.3 ± 11.6	121.1 ± 4.1	288.8 ± 3.9	123.0 ± 32.5

Magnitudes are expressed in kPa, angles in degrees; means ± SD for all steps in each session are shown. LD = lateral distal; LPD = lateral-posterior distal; LM = lateral mid-limb; LP = lateral proximal; PR = pressure; RS = resultant shear stress; RSang (θ) = resultant shear angle at the time of peak RS; NF = nonfunctional transducer.

Table 3d.
Peak interface stresses during stance phase: lateral region timings.

Session	Parameter	LD	LPD	LM	LP
TW812	PR	60.4 ± 22.7	NF	36.0 ± 22.9	65.9 ± 35.8
	RS	62.7 ± 27.2	NF	72.3 ± 18.2	22.8 ± 35.7
TW92	PR	24.9 ± 2.7	25.0 ± 10.8	36.6 ± 24.6	42.2 ± 34.9
	RS	94.4 ± 9.8	82.9 ± 17.3	59.1 ± 23.9	49.5 ± 40.9
WP1024	PR	34.3 ± 3.4	33.0 ± 2.6	70.0 ± 16.1	65.3 ± 39.5
	RS	77.8 ± 16.4	74.2 ± 31.5	30.9 ± 2.9	96.3 ± 0.4
WP125	PR	34.4 ± 9.4	32.6 ± 9.6	61.7 ± 24.8	50.7 ± 33.9
	RS	42.9 ± 36.2	43.4 ± 22.7	31.7 ± 7.2	86.0 ± 24.0

Timings are expressed in percentage of stance phase; means ± SD for all steps in each session are shown. LD = lateral distal; LPD = lateral-posterior distal; LM = lateral mid-limb; LP = lateral proximal; PR = pressure; RS = resultant shear stress; RSang (θ) = resultant shear angle at the time of peak RS; NF = nonfunctional transducer.

Table 3e.
Peak interface stresses during stance phase: posterior region magnitudes.

Session	Parameter	PD	PM	PF
TW812	PR	54.3 ± 4.7	81.7 ± 3.9	114.3 ± 12.6
	RS	25.7 ± 1.7	5.3 ± 1.1	10.4 ± 1.2
	RSang (θ)	101.1 ± 0.7	110.4 ± 30.5	212.8 ± 4.7
TW92	PR	72.7 ± 11.4	96.8 ± 8.4	105.3 ± 13.6
	RS	9.5 ± 1.7	NF	11.0 ± 1.1
	RSang (θ)	77.2 ± 6.0	NF	221.4 ± 5.7
WP1024	PR	59.9 ± 2.6	NF	43.0 ± 6.8
	RS	6.5 ± 2.6	NF	10.7 ± 1.2
	RSang (θ)	137.3 ± 11.9	NF	245.5 ± 12.6
WP125	PR	58.0 ± 5.8	88.6 ± 6.2	35.0 ± 6.0
	RS	7.1 ± 0.6	5.2 ± 0.8	10.5 ± 1.0
	RSang (θ)	79.4 ± 11.5	123.6 ± 26.2	280.0 ± 4.6

Magnitudes are expressed in kPa, angles in degrees; means ± SD for all steps in each session are shown. PD = posterior distal; PM = posterior mid-limb; PF = popliteal fossa; PR = pressure; RS = resultant shear stress; RSang (θ) = resultant shear angle at the time of peak RS; NF = nonfunctional transducer.

Table 3f.
Peak interface stresses during stance phase: posterior region timings.

Session	Parameter	PD	PM	PF
TW812	PR	31.1 ± 16.2	26.5 ± 11.5	33.0 ± 18.7
	RS	23.0 ± 2.2	74.1 ± 15.4	36.9 ± 17.3
TW92	PR	28.8 ± 12.5	22.4 ± 3.8	34.0 ± 20.7
	RS	23.1 ± 3.7	NF	53.5 ± 23.1
WP1024	PR	34.0 ± 3.5	NF	28.0 ± 6.3
	RS	48.1 ± 18.1	NF	27.2 ± 2.6
WP125	PR	33.9 ± 7.8	33.9 ± 14.5	22.6 ± 5.1
	RS	39.3 ± 13.7	85.5 ± 30.5	23.4 ± 5.0

Timings are expressed in percentage of stance phase; means ± SD for all steps in each session are shown. PD = posterior distal; PM = posterior mid-limb; PF = popliteal fossa; PR = pressure; RS = resultant shear stress; RSang (θ) = resultant shear angle at the time of peak RS; NF = nonfunctional transducer.

those at the PD site for TW but significantly less than those at the PD site for WP. Pressure and RS maxima at the LP, LM, LD, and LPD sites were significantly less than those at either AD sites (**Tables 3a** and **3c**).

Comparisons of sites in the lateral region with those in the posterior region showed some trends, but they were not consistent for all sessions. LD pressure maxima were significantly higher than PF pressure maxima for three of the four sessions (**Tables 3c** and **3e**). The RS maxima at LP, LM, and LD were lower than those at the PF site for three of the four sessions (**Table 3a, 3c**, and **3e**).

Timings of Maxima

Timings of maximal interface pressures and timings of maximal interface RS (and the corresponding RSang) were determined for each step, and the means and SD for all steps at each site in each session computed. Timings of maximal stance phase stresses were not simultaneous everywhere (**Tables 3b, 3d**, and **3f**). Some sites achieved maximal stresses during the first 50 percent of stance. The ALD, AMD, AMM, PD, PM, and PF sites demonstrated mean timings of maximal pressures during the first 50 percent of stance phase; timings of the maximal pressures were after the 1st pk at all except the PF site for WP1024 and WP125 and the AMD site for WP125. RS maxima were in the first 50 percent of stance phase at the following sites for all sessions: ALD, AMD, AMM, and PD. The maxima occurred after the 1st pk at all except the AMM and PF sites in WP1024 and the AMD and PF sites in WP125. The sites that achieved maximal pressure during the last 50 percent of stance were ALP and AMP. The PM site achieved maximal RS during the last 50 percent

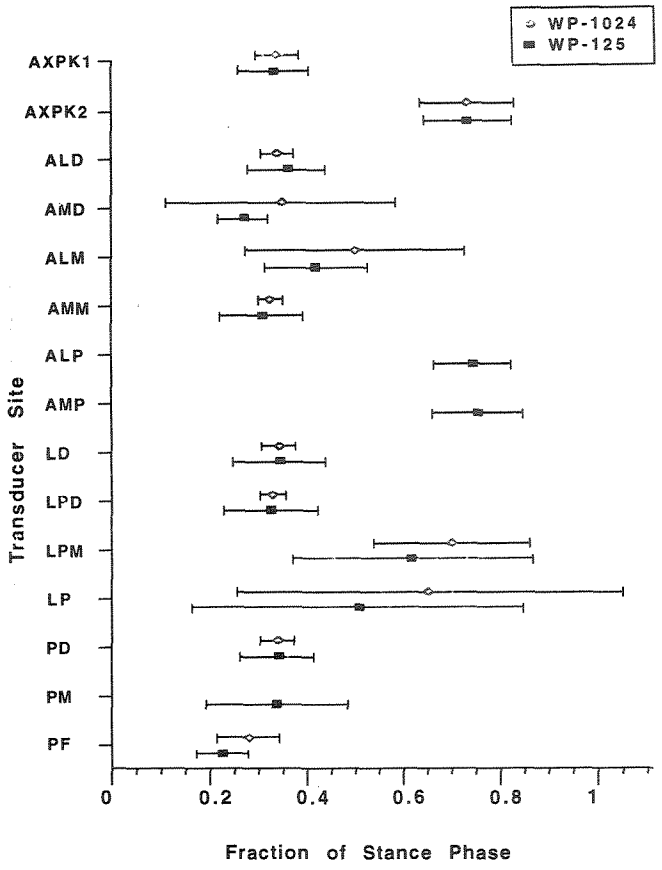

Figure 4.
Timings of stance phase pressure maxima for sessions WP1024 and WP125. Bars represent a positive and negative standard deviation from the mean for all steps within a session.

of stance phase. Sites that showed large SD in **Tables 3b, 3d**, and **3f** had interface stress-time curves of less distinct maxima than those with smaller SD.

There was not a gradual increase in the percent time into stance phase of interface stress maxima from AD sites to anterior mid-limb (AM) sites or AP sites. There were no significant differences between AD and AM maxima timings (percentage into stance phase) for any session. However, ALP and AMP pressure maxima occurred significantly later than AD or AM pressure maxima in all cases. Interestingly, there were differences between medial and lateral sides at anterior locations for WP (**Figure 4**). ALM pressure and RS maxima occurred later than AMM pressure and RS maxima respectively for both sessions for WP.

Posteriorly, pressure maxima were approximately simultaneous throughout the region. Mean time percentages into stance phase of pressure maxima for all posterior sites were within 11.6 percent of stance phase of each other for all posterior sites within each session. There was not a clear proximal-distal trend in timings of posterior pressure or RS maxima.

Pressures and Shear Stresses at First Peak and Second Peak in the Shank Axial Force-time Curve

It is important to note that for the stress magnitude results discussed above and presented in **Tables 3a, 3c,** and **3e,** stress maxima did not necessarily occur simultaneously. As shown in **Tables 3b, 3d,** and **3f** and as discussed in the *Timings of Maxima* section above, timings of the maximal stresses were different for the different sites and directions. Though the maxima data provide useful information, they do not provide a sense of the stress distribution at a single point in time. Thus, in this section, pressures and RS at two time points, 1st pk and 2nd pk, are considered because they are distinct events in a gait cycle, one early and one late in stance phase, at which high magnitude shank forces and moments occur. Maxima in shank force and moment data have been used as analysis reference points by other investigators, for example by committees developing standards for prosthetic componentry (29). Means and SD for all steps in each session of timings of 1st pk and 2nd pk were computed. For TW, the 1st pk occurred 21.8±1.8 percent and 21.5±4.0 percent into stance phase for session TW812 and TW92 respectively; the 2nd pk for the same sessions occurred at 77.3±2.6 percent and 78.7±1.1 percent into stance phase respectively. For WP, the 1st pk occurred at 31.5±4.8 percent and 30.7±6.9 percent into stance phase for WP1024 and WP125 respectively, while the 2nd pk for the same sessions occurred at 74.2±9.0 percent and 73.4±9.0 percent into stance phase respectively.

Interface pressures and RS at the times of the 1st pk and 2nd pk for all transducers were determined for each step and the means and SD for all steps at each site in each session determined. For each session, the sites that experienced the greatest stresses at the timings of the 1st pk (**Tables 4a–c**) were the same sites as those that experienced maximal stresses independent of time. For TW at the 1st pk, the highest pressures were at the ALD and AMD sites, while the highest RSs were at the ALD site. For WP at the 1st pk, the highest pressures were at the AMM site, while the highest RSs were at the AMD site (**Tables 4a–c**). The interface pressure and RS magnitudes at the 1st pk were lower than the maxima independent of

Table 4a.
Interface stresses at the time of the shank axial force first peak: anterior region magnitudes.

Session	Parameter	ALD	AMD	ALM	AMM	ALP	AMP
TW812	PR	138.9 ± 11.7	135.9 ± 8.1	73.6 ± 43.8	80.4 ± 7.5	2.8 ± 2.3	7.0 ± 2.3
	RS	59.3 ± 4.4	42.2 ± 3.3	10.9 ± 1.2	11.3 ± 2.9	0.7 ± 0.3	0.8 ± 0.4
	RSang (θ)	111.6 ± 1.3	91.7 ± 3.2	159.9 ± 17.6	90.2 ± 37.9	290.3 ± 25.4	26.4 ± 49.7
TW92	PR	197.2 ± 20.8	200.3 ± 27.5	97.8 ± 10.5	83.5 ± 15.4	NF	16.8 ± 4.3
	RS	47.4 ± 5.2	45.2 ± 13.1	8.9 ± 1.8	5.1 ± 3.5	NF	1.4 ± 0.4
	RSang (θ)	98.9 ± 2.3	92.7 ± 4.2	205.9 ± 13.5	322.4 ± 60.6	NF	349.2 ± 8.8
WP1024	PR	97.3 ± 8.3	109.4 ± 48.9	107.6 ± 0.1	151.9 ± 41.0	NF	NF
	RS	24.1 ± 2.7	32.9 ± 17.7	21.7 ± 3.0	3.6 ± 1.4	NF	NF
	RSang (θ)	17.1 ± 4.1	140.2 ± 16.8	54.1 ± 3.5	171.5 ± 41.1	NF	NF
WP125	PR	98.8 ± 9.7	117.5 ± 38.1	46.3 ± 3.9	147.2 ± 26.0	5.0 ± 5.5	28.8 ± 10.3
	RS	19.4 ± 1.5	27.7 ± 6.9	24.5 ± 2.4	14.4 ± 4.3	2.5 ± 0.9	6.4 ± 1.3
	RSang (θ)	73.0 ± 11.4	142.7 ± 7.3	95.1 ± 5.2	59.7 ± 13.6	12.4 ± 12.6	191.5 ± 8.1

Magnitudes are expressed in kPa, angles in degrees; means ± SD for all steps in each session are shown. ALD = anterior lateral distal; AMD = anterior medial distal; ALM = anterior lateral mid-limb; AMM = anterior medial mid-limb; ALP = anterior lateral proximal; AMP = anterior medial proximal; PR = pressure; RS = resultant shear stress; RSang (θ) = resultant shear angle at the time of peak RS; NF = nonfunctional transducer.

Table 4b.
Interface stresses at the time of the shank axial force first peak: lateral region magnitudes.

Session	Parameter	LD	LPD	LM	LP
TW812	PR	79.5 ± 0.1	NF	61.3 ± 6.1	4.3 ± 1.4
	RS	15.1 ± 1.3	NF	8.2 ± 1.0	2.2 ± 0.3
	RSang (θ)	139.2 ± 5.4	NF	203.5 ± 4.6	286.9 ± 13.2
TW92	PR	173.7 ± 19.7	88.4 ± 14.0	61.2 ± 8.2	10.0 ± 3.2
	RS	2.2 ± 1.0	2.6 ± 1.7	7.2 ± 0.9	1.3 ± 0.6
	RSang (θ)	146.7 ± 31.7	96.1 ± 26.4	215.8 ± 5.1	204.2 ± 74.2
WP1024	PR	85.6 ± 5.4	77.3 ± 3.8	47.7 ± 3.6	3.2 ± 0.9
	RS	5.6 ± 1.8	1.0 ± 0.3	7.9 ± 0.4	0.6 ± 0.2
	RSang (θ)	83.0 ± 12.2	309.2 ± 24.6	265.2 ± 1.6	138.8 ± 33.9
WP125	PR	95.7 ± 4.9	86.1 ± 7.1	58.2 ± 5.4	6.6 ± 2.0
	RS	5.0 ± 1.3	5.9 ± 1.2	4.7 ± 0.7	0.9 ± 0.3
	RSang (θ)	107.5 ± 10.6	121.0 ± 3.8	288.6 ± 3.5	132.6 ± 38.9

Magnitudes are expressed in kPa, angles in degrees; means ± SD for all steps in each session are shown. LD = lateral distal; LPD = lateral-posterior distal; LM = lateral mid-limb; LP = lateral proximal; PR = pressure; RS = resultant shear stress; RSang (θ) = resultant shear angle at the time of peak RS; NF = nonfunctional transducer.

time (**Tables 3a, 3c,** and **3e**) by 10.5 percent or less for all sessions except WP1024 RS at the AMD site, which was 50.2 percent lower.

For WP, from the 1st pk to the 2nd pk, there were medial-to-lateral shifts of the site of greatest pressure and RS. For WP1024, the site of greatest pressure shifted from AMM to ALM, while the greatest RS shifted from AMD to ALM. For WP125, the site of greatest pressure shifted from AMM to ALD, while the site of greatest RS shifted from AMD to ALM (**Tables 5a-c**). Thus, the results reflect the subject's lateral thrust at mid-stance. TW did not show this medial-to-lateral shift pattern.

For proximal sites in the anterior and lateral groups (ALP, AMP, LP), mean RSs at the 2nd pk were greater than those at the 1st pk, except at the LP site in WP125. It should be noted, however, that RSs at the LP site in WP125 were very low: 0.9±0.3 kPa at the 1st pk and 0.8±0.4 kPa at the 2nd pk. In all sessions, for three anterior (ALD, AMD, AMM) and three posterior sites (PD, PM, PF), mean pressures at the 2nd pk were less than those at the 1st pk.

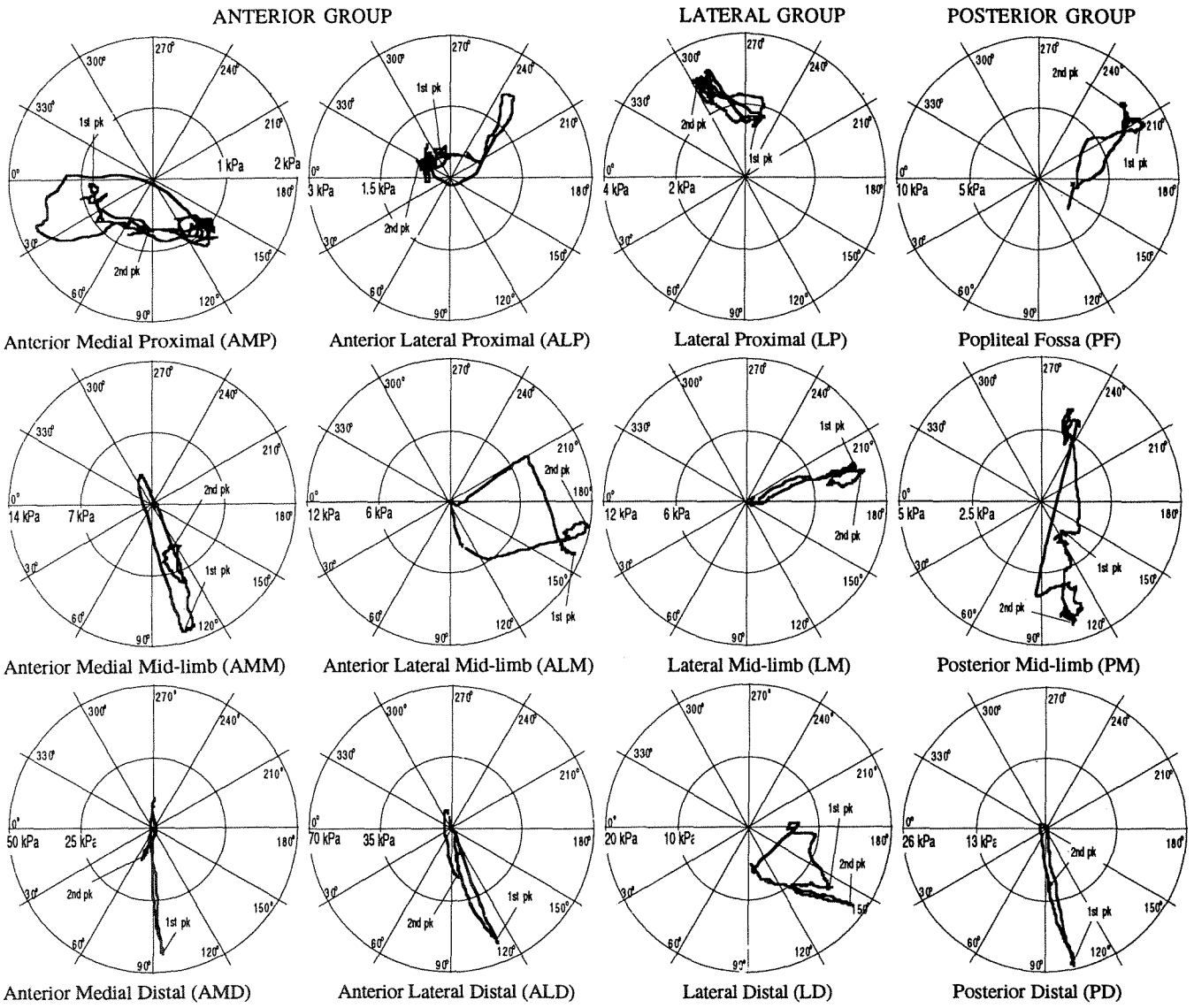

Figure 5.
Resultant shear stresses during stance phase for the anterior group (six sites, left side of figure), lateral group (three sites, central part of figure), and posterior group (three sites, right side of figure). Results are from a step during session TW812. Data are presented as polar plots where the radii are resultant shear stress magnitudes, and the angles are resultant shear stress directions.

Resultant Shear Stress Directions

RS directions are referenced to the horizontal shear axis as RSang in (**Figure 3**). Resultant shear directions changed over the course of stance phase, as shown in **Figure 5**. This figure illustrates the complex RS direction changes that can take place over one step. RS magnitudes and directions at the 1st pk can be drastically different from those at the 2nd pk at the same site.

At the 1st pk and 2nd pk and the interval in between, RSs at distal sites (PD, LD, AMD, and ALD) were directed more distally than proximally ($0^\circ <$ resultant shear angle $<180^\circ$) for all steps in all sessions (**Figure 6a–d** and **Figure 7a–d**). RSang of 0° and 180° indicate a RS in the transverse plane, and a RSang of 90° indicates a RS in the sagittal or frontal plane (depending on transducer location) and directed distally. Mean RSang at the 1st pk for all steps in each session are given in **Tables 4a–c.**

Table 4c.
Interface stresses at the time of the shank axial force first peak: posterior region magnitudes.

Session	Parameter	PD	PM	PF
TW812	PR	51.9 ± 4.7	79.9 ± 3.8	104.2 ± 13.2
	RS	25.4 ± 1.7	2.1 ± 0.9	9.4 ± 1.1
	RSang (θ)	100.9 ± 0.8	161.1 ± 43.0	207.2 ± 1.9
TW92	PR	69.4 ± 11.4	95.7 ± 8.2	96.2 ± 13.8
	RS	9.1 ± 1.5	NF	9.6 ± 1.2
	RSang (θ)	78.0 ± 6.0	NF	216.4 ± 8.1
WP1024	PR	59.2 ± 2.5	NF	34.7 ± 8.1
	RS	6.3 ± 2.7	NF	9.4 ± 1.3
	RSang (θ)	139.5 ± 10.0	NF	245.6 ± 11.9
WP125	PR	57.1 ± 6.0	87.5 ± 6.4	28.3 ± 6.6
	RS	6.9 ± 0.7	3.9 ± 1.1	9.2 ± 1.4
	RSang (θ)	79.0 ± 12.2	164.0 ± 26.6	282.1 ± 5.7

Magnitudes are expressed in kPa, angles in degrees; means ± SD for all steps in each session are shown. PD = posterior distal; PM = posterior mid-limb; PF = popliteal fossa; PR = pressure; RS = resultant shear stress; RSang (θ) = resultant shear angle at the time of peak RS; NF = nonfunctional transducer.

Table 5a.
Interface stresses at the time of the shank axial force second peak: anterior region magnitudes.

Session	Parameter	ALD	AMD	ALM	AMM	ALP	AMP
TW812	PR	55.8 ± 13.3	82.6 ± 7.3	78.5 ± 33.0	28.1 ± 10.8	3.5 ± 3.3	4.8 ± 1.6
	RS	29.4 ± 4.4	18.3 ± 4.5	11.0 ± 1.4	2.9 ± 1.2	0.7 ± 0.3	0.9 ± 0.3
	RSang (θ)	101.5 ± 5.1	79.2 ± 9.6	152.0 ± 14.2	92.0 ± 26.6	306.1 ± 36.4	90.6 ± 25.4
TW92	PR	137.1 ± 8.6	119.0 ± 19.3	82.2 ± 7.6	47.1 ± 10.6	NF	19.1 ± 8.3
	RS	31.0 ± 3.4	27.2 ± 11.9	8.2 ± 1.3	3.0 ± 2.1	NF	2.3 ± 0.5
	RSang (θ)	93.0 ± 2.1	89.2 ± 5.1	196.0 ± 17.5	358.3 ± 72.8	NF	40.4 ± 11.6
WP1024	PR	87.1 ± 8.2	34.3 ± 28.7	107.6 ± 0.1	41.2 ± 12.8	NF	NF
	RS	15.3 ± 4.2	18.8 ± 15.9	22.2 ± 2.4	5.5 ± 1.6	NF	NF
	RSang (θ)	35.6 ± 13.6	126.5 ± 41.0	76.9 ± 7.1	140.0 ± 7.2	NF	NF
WP125	PR	91.3 ± 10.9	40.7 ± 19.3	47.1 ± 3.3	71.1 ± 24.1	35.6 ± 11.2	50.2 ± 6.0
	RS	18.3 ± 2.2	11.2 ± 5.5	26.8 ± 2.3	10.5 ± 4.1	2.8 ± 0.7	7.4 ± 1.0
	RSang (θ)	88.6 ± 9.1	139.1 ± 9.0	103.8 ± 4.7	87.2 ± 11.7	75.1 ± 37.6	178.2 ± 19.2

Magnitudes are expressed in kPa, angles in degrees; means ± SD for all steps in each session are shown. ALD = anterior lateral distal; AMD = anterior medial distal; ALM = anterior lateral mid-limb; AMM = anterior medial mid-limb; ALP = anterior lateral proximal; AMP = anterior medial proximal; PR = pressure; RS = resultant shear stress; RSang (θ) = resultant shear angle at the time of peak RS; NF = nonfunctional transducer.

Those for the 2nd pk are given in **Tables 5a–c.** At the ALD site in all sessions, mean RSang at the 2nd pk were directed more distally than those at the 1st pk. Angular differences in mean RSang at the 1st pk compared with the 2nd pk at the ALD site were: 10.1° (TW812), 5.9° (TW92), 18.5° (WP1024), and 15.6° (WP125).

At the 1st pk and 2nd pk and the interval between them, RS directions at most of the proximal sites in the lateral and posterior groups were directed more proximally than distally. For the stance phase interval between the peaks, mean RS directions at LM and PF sites in all sessions were between 180° and 360°. RSang of 180° and 360° indicate a RS in the transverse plane, and a RSang of 270° indicates a RS in the sagittal or frontal plane (depending on transducer location), directed proximally. Mean RSang at the LM, PF, and LP sites are shown in **Tables 4b,c,** and **5b,c**. LP sites on TW showed RSangs that were more proximally directed than distally directed. For WP, RSangs at the LP site were directed distally in both sessions.

RSs at AD sites were directed toward the apex of the socket in some but not all sessions. Mean ALD and mean AMD RSs at the 1st pk were directed toward the socket apex in all sessions for WP but for TW mean AMD, RSs

Table 5b.
Interface stresses at the time of the shank axial force second peak: lateral region magnitudes.

Session	Parameter	LD	LPD	LM	LP
TW812	PR	79.6 ± 0.1	NF	55.8 ± 6.9	1.6 ± 0.8
	RS	17.4 ± 1.3	NF	9.6 ± 0.8	2.9 ± 0.1
	RSang (θ)	139.8 ± 3.5	NF	204.7 ± 5.2	298.7 ± 4.0
TW92	PR	113.6 ± 8.0	73.8 ± 9.6	57.6 ± 2.7	10.5 ± 4.2
	RS	2.8 ± 1.0	4.8 ± 1.4	7.8 ± 0.7	1.5 ± 0.6
	RSang (θ)	99.6 ± 16.6	72.5 ± 9.1	217.4 ± 3.5	357.7 ± 15.3
WP1024	PR	75.5 ± 5.6	69.1 ± 4.0	50.6 ± 7.1	8.7 ± 3.2
	RS	6.0 ± 1.8	0.8 ± 0.4	4.9 ± 0.7	1.4 ± 0.6
	RSang (θ)	81.2 ± 11.2	318.6 ± 29.1	261.1 ± 2.5	77.2 ± 24.2
WP125	PR	89.6 ± 4.9	80.6 ± 6.4	60.1 ± 8.0	12.6 ± 3.7
	RS	4.9 ± 1.4	5.9 ± 1.0	3.0 ± 0.8	0.8 ± 0.4
	RSang (θ)	105.2 ± 10.4	121.1 ± 2.9	279.1 ± 4.5	71.8 ± 68.1

Magnitudes are expressed in kPa, angles in degrees; means ± SD for all steps in each session are shown. PR = pressure; RS = resultant shear stress; RSang (θ) = resultant shear angle at the time of peak RS; NF = nonfunctional transducer.

Table 5c.
Interface stresses at the time of the shank axial force second peak: posterior region magnitudes.

Session	Parameter	PD	PM	PF
TW812	PR	47.4 ± 3.5	70.3 ± 5.3	85.0 ± 10.0
	RS	11.4 ± 1.8	5.2 ± 1.2	8.4 ± 0.9
	RSang (θ)	98.2 ± 3.4	106.4 ± 12.2	218.1 ± 4.3
TW92	PR	60.6 ± 7.2	79.3 ± 5.1	88.1 ± 13.9
	RS	4.3 ± 1.1	NF	10.4 ± 1.3
	RSang (θ)	72.8 ± 6.3	NF	221.6 ± 6.5
WP1024	PR	52.9 ± 2.8	NF	20.1 ± 2.9
	RS	6.2 ± 2.4	NF	4.8 ± 0.6
	RSang (θ)	135.6 ± 11.3	NF	244.9 ± 11.3
WP125	PR	53.5 ± 5.3	82.7 ± 6.8	19.5 ± 2.1
	RS	6.7 ± 0.6	3.8 ± 1.1	6.9 ± 0.5
	RSang (θ)	79.8 ± 11.3	158.9 ± 27.8	287.6 ± 4.0

Magnitudes are expressed in kPa, angles in degrees; means ± SD for all steps in each session are shown. PD = posterior distal; PM = posterior mid-limb; PF = popliteal fossa; PR = pressure; RS = resultant shear stress; RSang (θ) = resultant shear angle at the time of peak RS; NF = nonfunctional transducer.

at the 1st pk were directed 1.7° to 2.7° off the vertical (vertical is 90°) and directed away from the socket apex (**Table 4a**). At the 2nd pk, all ALD and AMD sites had mean RSs directed toward the apex of the socket in all sessions.

Though at the 1st pk, anterior RS directions were not always consistently toward the apex of the socket as in previous interface shear stress studies on persons with TTA (12,15), further analysis of the data suggests that the skin was still loaded in tension at AD sites. Consider the differences in horizontal shear stresses between the ALD and AMD sites at the times of the 1st pk and 2nd pks: means and SD for all steps in each session are shown in **Table 6a**. In all sessions, differences in horizontal shear stress between adjacent anterior sites indicate the skin was in tension across the tibial crest at AD locations. It is important to note that the magnitudes represent only the differences in shear stresses in the transverse plane (differences in horizontal shear stress) between two measurement sites on the socket, not necessarily the tension in the skin, since skin between the two transducer sites was not isolated from surrounding skin. The point here is that the data indicate the skin was in tension across the tibial crest at distal locations.

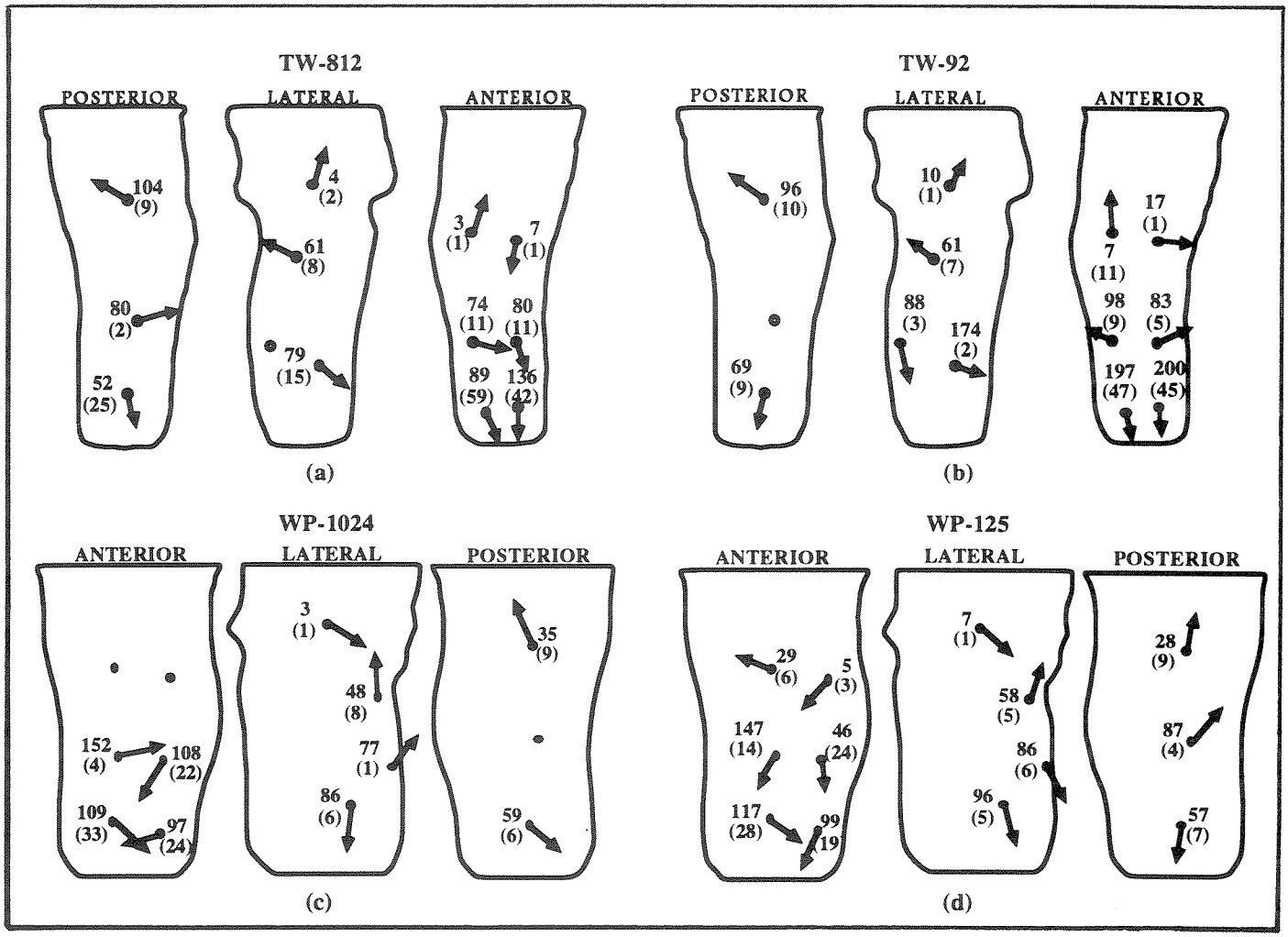

Figure 6.
Interface stress maxima (means for all steps in each session) at the time of the shank axial force first peak. Pressures (in kPa) are shown next to the arrows; resultant shear stresses (in kPa) are in parentheses. Arrows indicate resultant shear stress directions. Sites at which transducers did not function properly are shown with open circles. a: Session TW812. b: Session TW92. c: Session WP1024. d: Session WP125.

Table 6a
Horizontal shear stress differences at anterior distal sites at the time of the shank axial force first and second peaks.

Session	1st pk Lateral/Medial	2nd pk Lateral/Medial
TW812	+20.5 ± 3.1	+9.0 ± 2.7
TW92	+4.8 ± 2.6	+1.4 ± 3.1
WP1024	+45.1 ± 10.3	+18.2 ± 8.1
WP125	+27.7 ± 8.9	+8.7 ± 5.7

Resultant shear stress differences in kPa between adjacent anterior sites for all steps in each session. Means ± SD are calculated at the time of the shank axial force first and second peaks. A '+' indicates tension, a '−' compression, between sites.

For the vertical direction, the data indicate that in most cases the skin was not in tension between adjacent anterior sites (**Table 6b**). Differences in vertical shear stresses at the 1st pk and 2nd pk usually did not indicate tension but instead indicated compression in the plane of the skin between sites. Exceptions were between the mid-limb and distal transducers on the anterior lateral side for WP1024 and WP125 and between the mid-limb and proximal sites for TW92. Skin between the mid-limb and distal transducer sites was in tension during the 1st pk and 2nd pk and the interval between them for all steps in those sessions. Again, it is important to note that the magnitudes represent only the differences in vertical shear stresses between adjacent trans-

Table 6b.
Vertical shear stress differences at anterior sites at the time of the shank axial force first and second peaks.

	1st pk				2nd pk			
	Mid-Limb/Distal		Mid-Limb/Proximal		Mid-Limb/Distal		Mid-Limb/Proximal	
Session	Lateral	Medial	Lateral	Medial	Lateral	Medial	Lateral	Medial
TW812	−51.3 ± 6.4	−31.5 ± 5.6	−4.4 ± 3.4	−10.5 ± 4.2	−23.3 ± 5.8	−15.2 ± 4.9	−5.7 ± 2.7	−1.9 ± 1.2
TW92	−50.9 ± 5.2	−48.7 ± 11.1	NF	+3.5 ± 4.9	−33.3 ± 5.6	−28.4 ± 10.8	NF	+2.7 ± 3.2
WP1024	+10.3 ± 3.5	−21.5 ± 17.7	NF	NF	+13.3 ± 3.4	−13.7 ± 16.1	NF	NF
WP125	+6.1 ± 2.4	−4.0 ± 5.9	−23.8 ± 2.2	−13.4 ± 4.3	+7.9 ± 2.7	+3.0 ± 2.1	−23.8 ± 2.6	−10.1 ± 5.3

Resultant shear stress differences in kPa between adjacent anterior sites for all steps in each session. Means ± SD are calculated at the time of the 1st pk and the 2nd pk. A '+' indicates tension, a '−' compression, between sites. NF = nonfunctioning transducer.

ducer sites, not necessarily the magnitude of tension (or compression) in the skin. Thus, the data suggest that horizontal tension occurred at the AD end of the residual limb in all sessions; vertical tension occurred between sites on the anterior surface in only a few selected cases.

Waveform Shapes

Pressures at different posterior sites were similar in shape to each other, as noted in previous investigations (30). Though magnitudes at different sites varied, the waveform shapes when normalized were very similar (**Figure 8a**). The ratios between the pressures achieved at the 1st pk and those at the 2nd pk were higher at the PF site than at the PD site in three of the four sessions. Ratios at the PF sites were 1.23, 1.09, 1.73, and 1.45, and ratios at the PD sites were 1.09, 1.15, 1.12, and 1.07 for sessions TW812, TW92, WP1024, and WP125, respectively. Except at the most proximal site, pressure-time curves in the lateral region were also similar in shape to each other and were similar to those at the posterior sites (**Figure 8b**). RSs, however, did not show consistently-shaped waveforms at sites within a group. An example is shown in **Figure 9.**

At AM and AD sites, there were typically "loading delays" between heel contact and the time the interface stresses began to increase (**Figure 9**). This trend was noted previously at anterior sites on other subjects (15). Loading delays were typically less than 15 percent of stance phase in duration and tended to occur only in the anterior region.

Temporal Changes

For each subject, mean interface stresses in one session were compared with those from the other session. For all transducers that functioned properly in both sessions for each subject, mean maximal stance phase pressures were significantly different at all sites except some mid-limb sites for TW (ALM, AMM, and LM) and some mid-limb and distal sites for WP (AMM, ALD, AMD, and PD; **Figures 10a–d**). The significant differences in mean maximal pressures in kPa for all steps between TW92 and TW812 were: ALD +69.8, AMD +83.8, AMP +15.1, LD +100.9, LP +7.2, PD +18.4, PM +15.1, and PF −9.0; the significant differences between WP125 and WP1024 were: ALM −55.6, LD +10.7, LPD +9.1, LM +8.1, LP −10.1, and PF −8.0. For RS maxima, all sites showed significant differences between sessions for TW except PF; for WP, LD, PF, and PD locations were the only sites that did not show significant differences. The significant differences in mean maximal RS in kPa for all steps between TW92 and TW812 were: ALD −11.3, AMD +5.0, ALM −2.3, AMM −4.8, AMP +1.0, LD −13.4, LM −1.5, LP −1.0, PD −16.2. The mean maximal RS differences between WP125 and WP1024 were: ALD −3.6, AMD −36.1, ALM +4.8, AMM +8.8, LPD +4.7, LM −3.2, LP −2.2. In addition, at the times of the 1st pk and 2nd pk and the interval between them, RSs at ALM, AMM, AMP, LM, and PF sites were more proximally directed for TW92 than for TW812 (**Figure 6a** and **b**, and **Figure 7a** and **b**).

It is interesting to consider the trends in maximal interface stress magnitudes for the two sessions. For TW, all distal pressures were significantly higher in session TW92 than in TW812, consistent with his complaining that he was "bottoming out" during TW92. In general, mean stance phase pressure maxima were higher, and mean RS maxima were lower in magnitude in TW92.

For WP, session differences occurred but trends were not as consistent as in TW. Mean maximal pressures in the lateral group at LM, LPD, and LD sites were increased (8, 9, and 11 kPa, respectively) for WP125 compared with WP1024, and AM mean maximal RSs were increased (9 and 5 kPa at the AMM and ALM sites,

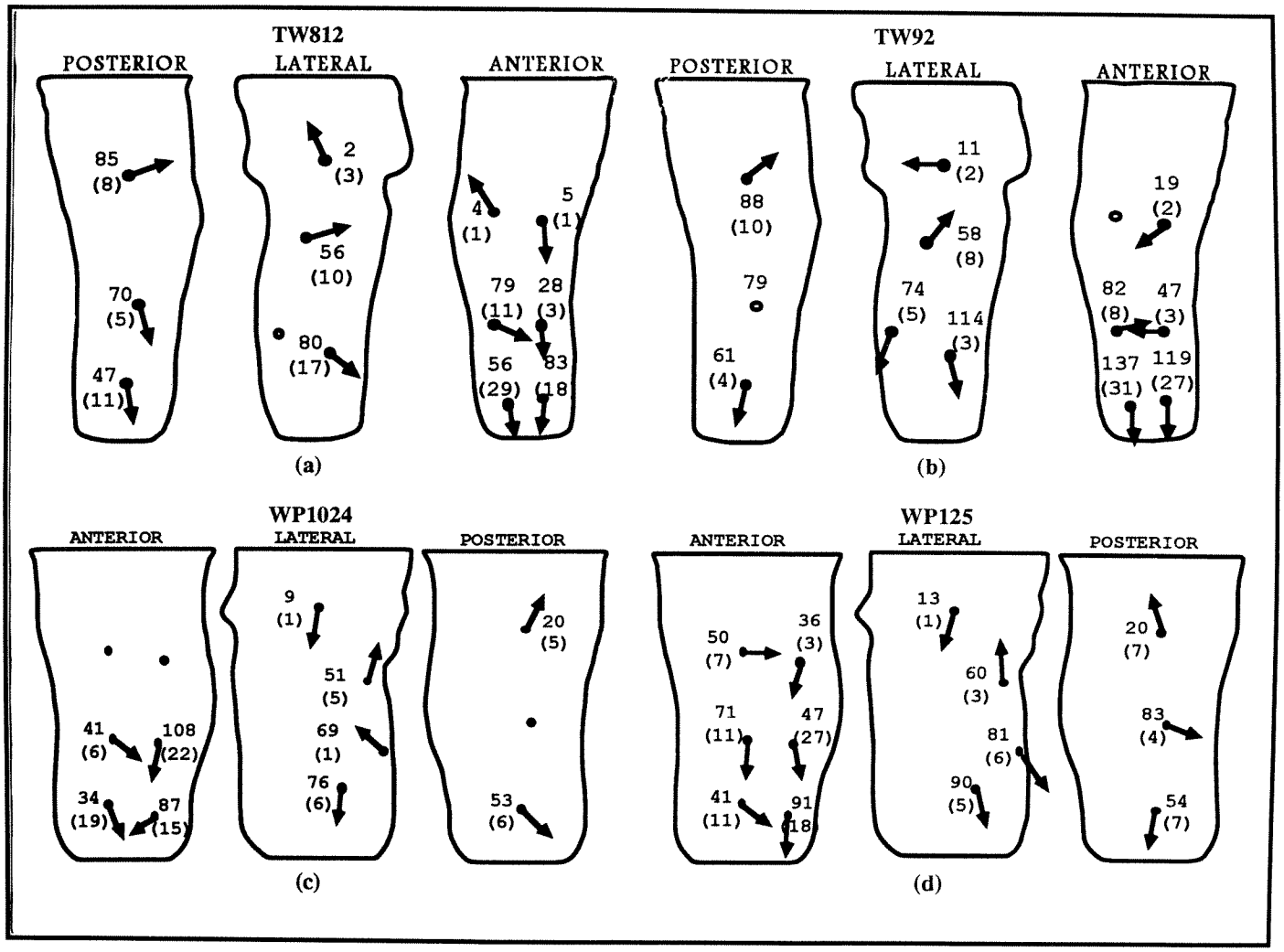

Figure 7.
Interface stress maxima (means for all steps in each session) at the time of the shank axial force second peak. Pressures (in kPa) are shown next to the arrows; resultant shear stresses (in kPa) are in parentheses. Arrows indicate resultant shear stress directions. Sites at which transducers did not function properly are shown with open circles. a: Session TW812. b: Session TW92. c: Session WP1024. d: Session WP125.

respectively). Mean maximal ALM pressures and mean maximal AMD RSs were much lower (56 and 36 kPa, respectively) for WP125 than for WP1024.

DISCUSSION

This research expands upon previous studies in TTA interface mechanics, investigating the consistency of findings discussed in the literature as well as addressing new issues. The data are unique in that stresses were measured in 3 orthogonal directions at many more sites, 13, than in previous 3-D interface stress studies: 4 (12,15) or 5 (13).

The style, design, and fit of the instrumented prostheses need to be considered in analysis of these data, as these prostheses were different from the subjects' regular artificial limbs in three principal respects. First, sockets were of greater mass with their added 0.41 kg of transducers and a 0.36 kg instrumented pylon was used during data collection rather than the normal Seattle ankle or FlexFoot. Second, the instrumentation required the sockets at the transducer mount sites to be modified to flat surfaces, though attempts were made to minimize the degree of modification by requiring that transducers be placed only at relatively flat locations. The greatest degree of modification was on the posterior surface, but as the pos-

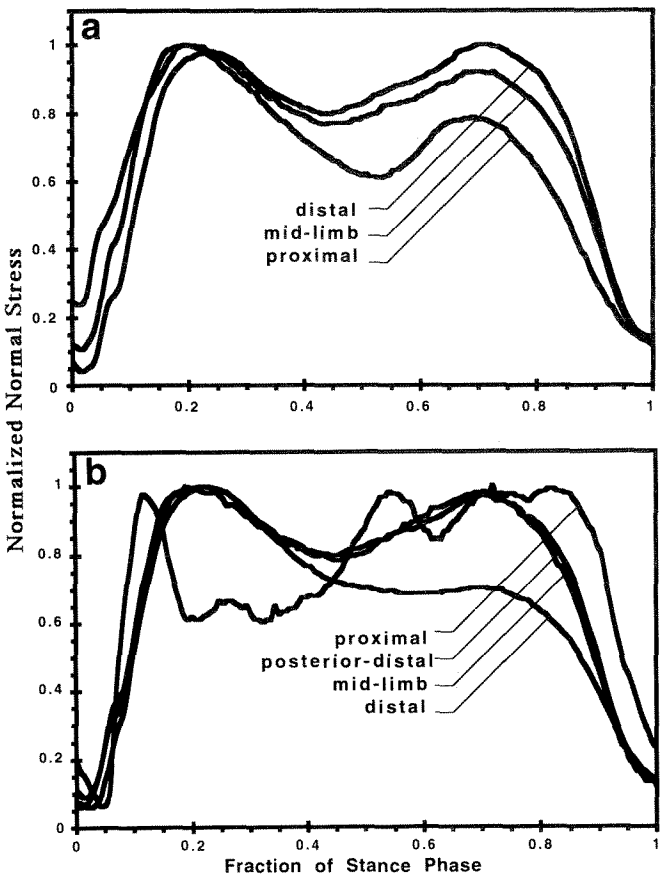

Figure 8.
Interface pressures normalized with respect to their maximal stance phase magnitudes at each site are shown. a: Pressures at posterior sites in session TW92. Proximal refers to the PF site. b: Pressures at lateral sites in session TW92.

terior region of the residual limb is soft tissue with no immediate underlying bone, the socket shape changes will have a less pronounced effect there than at sites with thin soft tissue over bone. Third, it is clear from the comments by TW and the prosthetists that both residual limbs underwent shrinkage between the time the sockets were fabricated and the studies conducted. Adding socks was not possible because of their effects on performance of the instrumentation. The prosthetists deemed the fit here acceptable to conduct short-term ambulation studies but sub-optimal. Residual limb shrinkage is normally an issue in prosthetic design and fitting: the fits reported here are not atypical. To try to overcome variability in the gaits introduced by these three factors, at least one preliminary session was conducted on each subject.

In interface stress studies discussed in the literature, descriptions of socket fit are rarely included. Where

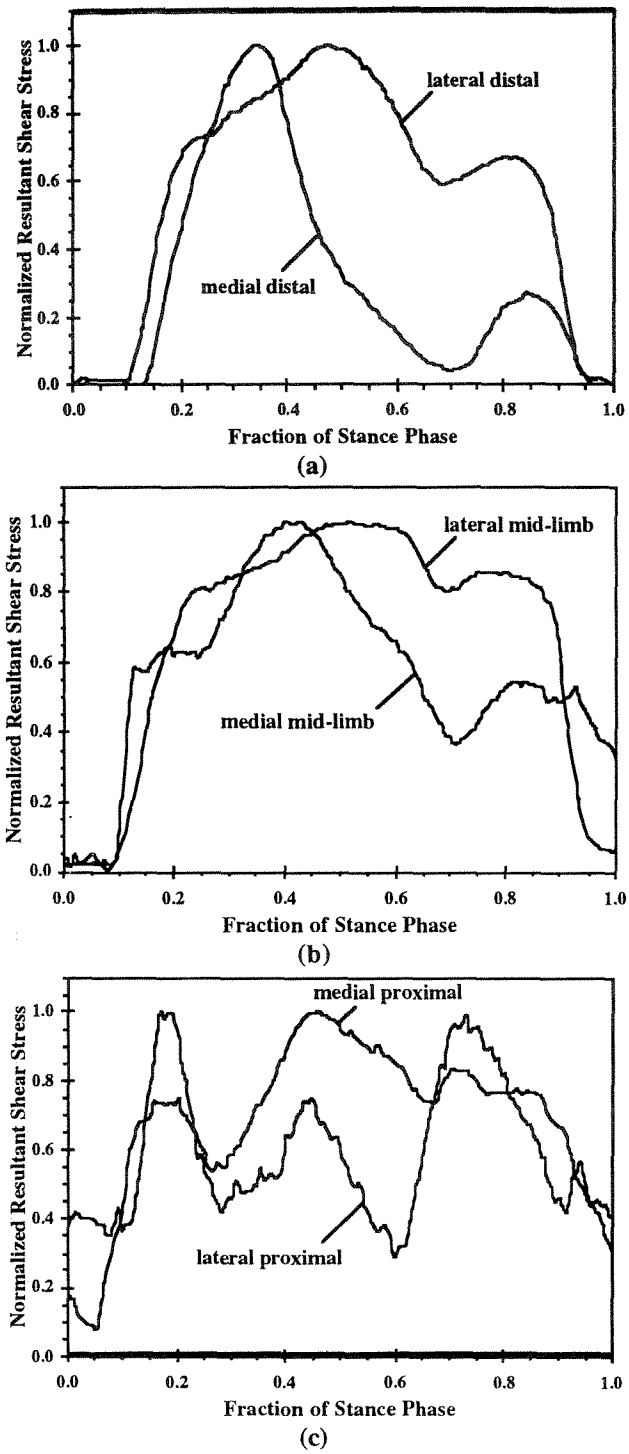

Figure 9.
Interface resultant shear stresses normalized with respect to their maximal stance phase magnitudes at each site are shown for anterior sites from session TW812. a: Anterior lateral distal and anterior medial distal sites. b: Anterior medial mid-limb and anterior lateral mid-limb sites. c: Anterior lateral proximal and anterior medial proximal sites.

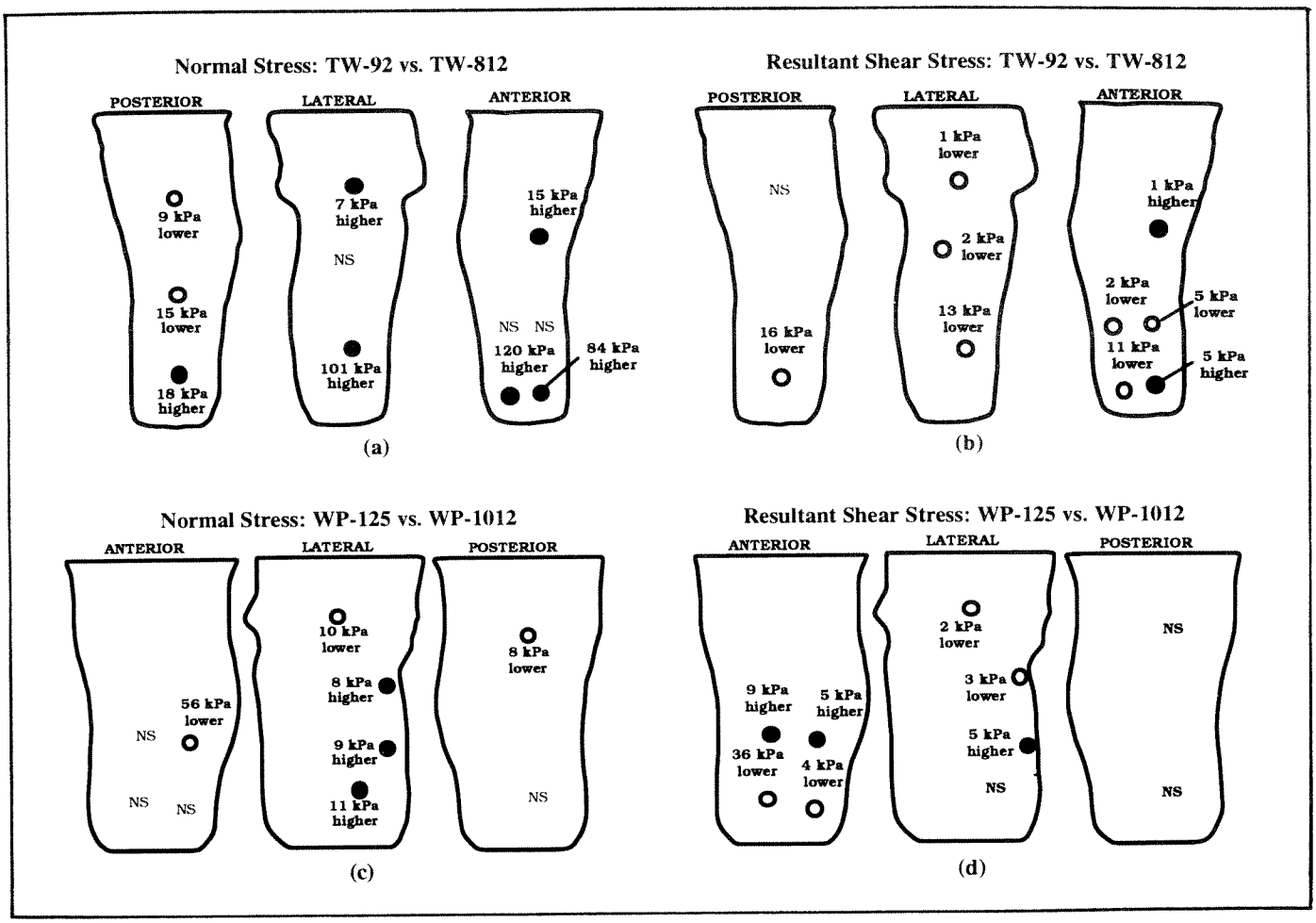

Figure 10.

Peak stance phase interface stresses for different sessions are compared. A filled circle indicates a significantly higher stress; an open circle indicates a significantly lower stress. NS = no significant difference. a: Pressures in session TW92 are compared with those in session TW812. b: resultant shear stresses in session TW92 are compared with those in session TW812. c: Pressures in session WP125 are compared with those in session WP1024. d: resultant shear stresses in session WP125 are compared with those in session WP1024.

transducers were taped onto the residual limbs or sockets, no socket modification was necessary (4–9,14); presumably subjects used their regular acceptably fitting prostheses. Winarski (11) explains that his subjects were in the process of being fitted. Where transducers were mounted in new socket walls, Appoldt (1–3) and Bielefeldt (10) state that the sockets were "well-fitting." Appoldt made duplicates of the subjects' regular sockets for use in his studies and Williams (13) made a new socket specifically for the study. Sanders (12,15) required new sockets slightly smaller than normal since no socks were worn in the studies.

It is important to recognize that some transducers did not function properly in some sessions. The described stress comparisons among sites hold for all collected data, but this limitation in completeness of the data sets must be recognized.

Pressure and Shear Stress Magnitudes

Maxima and Magnitudes at the First Peak and Second Peak in the Shank Axial Force-time Curve

The maximal interface pressures and RSs at a site are the greatest stresses to which the tissues are subjected during the stance phase of walking. Thus, with all other factors being equal, they are the stresses that pose the greatest risk of damage to tissues at the transducer sites during ambulation. The finding in this study that AD or AM sites received greater stresses than those at the level

of the tibial condyles is consistent with Pearson's results on 10 subjects with TTA, using PTB prostheses at neutral alignment (8). In our previous investigations, however, PM and LM sites experienced greater pressures and RS than the AD (30). It is expected that the high AD and AM pressures reported here are in part a reflection of residual limb shrinkage. A loose socket tends to concentrate stresses anterior distally.

Though the trends in the distribution of stresses at anterior sites here are similar to those reported in Pearson's study, his interface pressure measurements were of larger magnitude than those presented here or in previous studies from our laboratory on other subjects (12). Pearson reported that stance phase pressure maxima at the AD site averaged 289±194 kPa. At the lateral tibial condyle site, pressures averaged 122±100 kPa; at the medial tibial condyle site, they averaged 50±40 kPa (8). In our previous study, pressure maxima at AP sites ranged from 30.9 kPa to 103.2 kPa while those at AD locations ranged from 53.4 kPa to 139.5 kPa (12). In the present study, pressure maxima at AD and AM sites ranged from 52.2 kPa to 223.8 kPa while those at AP sites ranged from 14.1 kPa to 54.0 kPa. Though differences between these studies may have been due simply to subject differences (note that SD for pressure maxima in Pearson's study were quite large), there are two other explanations to consider. First, Pearson measured specifically at sites expected to be high load-bearing locations, not restricting transducer location to flat sites as done here. Thus, the pressures may have simply been greater at those selected sites. Second, he used Kulite™ disk-shaped sensors, 3.18 mm in diameter, 0.76 mm thick, placed between the skin and liner, with the attached cables exiting at the socket brim. As shown in a transducer evaluation study by Patterson (31) stiff sensors, even if very thin, tend to be susceptible to error when sandwiched at an interface (i.e., when no recession is made for the transducer). The sensor protrudes into the skin, tending to concentrate stresses at its edge and distorting the uniformity of the stress distribution on its surface. Thus, presence of the sensor distorts the measurement of interest. The stress distortion problem tends to be worse (more error) at thin skin sites over bone (e.g., AD over the tibial flares) than at soft underlying tissue locations (e.g., PM). Thus, Pearson's high pressures and large SDs may have been due, in part, to an instrumentation limitation.

Pressure and RS maxima reported here did not differ substantially from our previous studies using a different interface/transducer configuration: holes cut in Pelite liners bonded to the inside socket surfaces, with Pelite disks attached to the ends of the transducers. Thus, skin-liner stresses were measured without socks (12,15). In the present study, sock-socket interface stresses were measured; no liner was worn. A reduction of RS magnitudes would be expected in this study because the coefficient of friction between sock and transducer is lower than that between skin and Pelite. In addition, the sock provides in-plane tension, reducing the tension in the skin. A converse argument, however, is that because there is no liner to help distribute the shear stresses, RSs are expected to be higher. Results show that RS magnitude with the Pelite configuration ranged from 5.0 kPa to 40.7 kPa (12) while those here ranged from 1.5 kPa to 66.1 kPa. Because the ranges are similar, it is possible that these two factors did not have significant effect or countered each other to produce minimal net change; alternatively, the differences in socket designs and quality of fit between the two groups of subjects countered either or both effects.

Interface stresses at the 1st and 2nd pks provide a sense of the distribution of stress at two points in time in stance phase. Stresses were not at their maxima during the 1st pk, but were close, within 10.5 percent at all sites except the RS at the AMD site for WP 1024, which was 50.2 percent lower. Thus, it should be recognized in prosthetic FE analysis that modeling stresses at the time of the 1st pk is not necessarily modeling the time of highest interface stresses at all sites.

WP's medial-to-lateral shift of the site of peak pressure and RS on the anterior surface from the 1st pk to the 2nd pk reflects his lateral thrust at mid-stance noted by the prosthetists (**Table 1**). This might also be indicative of a loose socket, since stresses tended to be concentrated distally on the lateral surface.

Timings of Peaks

Timings of interface stress maxima are one of several factors important to residual limb tissue mechanics. The relative magnitudes and directions of interface stresses affect the pressure and shear stress gradients and tension in the plane of the skin. High pressure and shear stress gradients and in-plane tension are expected to be more damaging to skin than an equivalent force uniformly distributed with no tension. The lack of simultaneous timings of stance phase interface stress maxima at all sites in the same step have been reported by Pearson (8) and Sanders (15); however, because so few sites were monitored in those studies, few statements concerning stress distributions could be made.

In all sessions in this study, maximal stresses at the AD, PM, and PF locations occurred in the first 50 percent of stance phase. This is a reasonable result since the AD/posterior proximal (PP) force couple helps to avoid both knee hyperextension and active knee flexion in stance phase. A proper socket design and alignment will stabilize the knee in near extension and avoid hyperextension and active flexion during stance. The finding that AP stresses maximized later than those at AD locations in the same step was expected, because of the combined effects of: 1) resistance to knee bending moment at heel contact (encouraging high stresses AD); and 2) the knee extension moment occurring at about 50 percent of stance when the center of gravity advances anterior to the knee center (encouraging high stresses AP). There was not a clear distal-to-proximal progression of maxima timings on the anterior surface, suggesting there was not a "rolling" action of the socket on the anterior residual limb surface but instead a more abrupt change in stress distribution. Again, this result may have been a reflection of the loose socket fit.

Posteriorly, the consistent timings of peak pressures at all three posterior sites (PD, PM, and PF, within a window of 11.6 percent of stance phase for each session) was expected because of the large soft tissue mass (gastrocnemius and soleus muscles) in the region. This region makes an important load-bearing contribution during weight-acceptance. The soft tissue mass helps to create a more uniform and low frequency content waveform in the region, resulting in consistent peak interface stress timings. Thus, unlike the anterior surface where timings of maximal stresses ranged over most of stance phase, the posterior surface was more consistent within a step in its timings of stress maxima.

Resultant Shear Stress Directions

RSs are important because of their effects on the risk of tissue breakdown. Shear stress reduces the pressure necessary to cause blood flow occlusion (32). The magnitudes and directions of shear stresses affect the stress distribution in the soft tissues, particularly the tension in the skin.

The RSang being directed more distally at the 2nd pk than at the 1st pk at ALD and AMD sites is expected. With the ground reaction force applied near the toe during the time of the 2nd pk, a higher sagittal plane bending moment of the socket on the residual limb is induced, tending to push the residual limb downward deeper in the socket at AD sites.

The finding of proximally directed RSs at most of the proximal sites and at some mid-limb locations is interesting, because during stance phase the skeleton moves downward in the socket, as shown by x-ray analysis (33). The RSs on the socket would be expected to be distally directed. A possible explanation for their proximal direction is soft tissue and fluid displacement. During stance phase, once the residual limb was deep into the socket (at the end of "pistoning"), the soft tissue could not displace laterally because of the socket wall. There was minimal space available distally, and tension in the distal skin would prevent significant downward displacement. The only alternative was for the soft tissue to displace proximally toward the socket brim, resulting in proximally directed RSs at those sites.

The finding of proximally directed resultant shear stresses at some sites in this study is consistent with results reported on persons with transfemoral amputation by Appoldt (3). He used transducers mounted in the socket wall flush with the interface as in this study, though his shear transducer was unidirectional rather than bidirectional. By mounting it with its principal axis oriented proximal-distal, Appoldt could determine whether shear stresses were directed proximally or distally within a step. His explanation for the upwardly directed shear ("tangential") stresses was similar to that above: "When driven into the socket during the stance phase, such a piston action might force sections of flesh remote from the femur to rise, reflecting conservation of mass considerations (3)."

In previous studies on persons with TTA, RSs with a proximally directed vertical component were found at some AP locations in some sessions (30). At PP and lateral sites in those studies, transducers were positioned more distally than in this study so as to avoid interfering with the suspension system (sleeve). In the present study, holes cut in the neoprene sleeves allowed mounts to project through them, permitting measurements at more proximal locations. Thus, the lack of proximally directed RSs at lateral and posterior sites in previous studies, but their presence here may reflect transducer location. Alternatively, proximally directed RSs here may have been a reflection of the loose socket fit. Interface stress studies using at least two sockets, each of a different fit, on each subject would need to be conducted to evaluate RS direction dependence on socket fit.

The findings of proximally directed RSs at some sites in this and our previous studies and in Appoldt's investigations lend experimental support to a FE model-

ing issue raised by Vannah (34) on the resistance to external load offered by 'narrow containment' of the soft tissue. Narrow containment occurs when a narrow layer of soft tissue is constrained between two similarly shaped, relatively rigid surfaces, as between the bone and socket in lower limb prostheses. The spacing between the surfaces is narrow in relation to their overall dimensions. If the tissue was assumed isotropic, incompressible, and linearly elastic, FE analysis indicated that under compression it "flows" out of the containment toward the free edge—in the case of a prosthetic socket, toward the proximal brim—inducing shear stresses near the free edge directed outward. This result is consistent with proximal RS directions measured in this study. The degree of bulging and the magnitude of the reaction forces were shown to be very sensitive to the Poisson's ratio used in the FE model to control the near incompressibility of the soft tissue. Vannah suggests that, in addition to the accepted mechanisms of soft tissue compression and direct load transfer to tolerant areas, the shear stresses resulting from near incompressibility may also contribute resistance to external loads.

In previous studies of subjects with TTA, interface RSs were directed toward the apex of the socket at most of the anterior sites (12). Data from three subjects showed horizontal shear stresses (interface shear stress in a transverse plane) on the transducers at AD regions that tended to be so directed. This result was a reasonable finding, since the tibia was forced into the apex during most of stance phase by the AP force applied at the base of the socket (measured by an instrumented pylon). Thus, the socket was forced posteriorly relative to the residual limb; this is likely to put the skin over the crest of the tibia in tension (in the plane of the skin).

At AD locations in this study, consistent with previous findings, the differences in RSs across the tibial crest suggest that skin tension was induced between AMD and ALD sites. Skin tension is important because of its role in skin breakdown, particularly when skin mobility is diminished by scars or grafts. Shear stresses in opposite directions at sites less than 5 cm apart have also been reported by Appoldt (3) and their potential importance to tension in the flesh and pain identified. Tension will stress the fibrous components of the dermis as well as intercellular connections in the epidermis. Tibial extension contributes toward AD skin tension by moving the distal tibia anteriorly relative to the socket. The proximal tibia, however, is much closer to the center of rotation at the knee; thus, tibial extension contributes relatively little to thrusting the tibia anteriorly at AP locations. This may help to explain why tension was consistently observed at all AD sites but not at all AP ones.

Calculations of differences in vertical shear stresses between adjacent sites in this study suggest in-plane compression, as opposed to in-plane tension, was induced in the proximal-distal direction at most anterior sites. In-plane compression, unless pinching occurs, is not particularly threatening to the skin. However, for anterior regions that did show tension in the vertical direction (a positive difference in vertical shear stress), as well as in the horizontal direction (a positive difference in horizontal shear stress) within a local region, biaxial loading, which is a threatening skin loading configuration, is induced. Skin under tension will absorb less energy in that direction before failure if there is tension in the orthogonal direction in the plane of the skin. Carefully conducted biaxial loading studies on excised rat skin by Lanir (35) demonstrated this result. The biaxial loading condition noted here in some sessions may have been due to an improper socket fit occurring as a result of residual limb shrinkage. A well-controlled study investigating socket shape change effects on interface stresses would need to be conducted to evaluate effects of fit on interface stress distributions and the occurrence of in-plane biaxial loading.

Waveform Shapes

The shapes of interface stress waveforms can have important implications for dynamic analysis of the residual limb and socket, particularly FE modeling. Waveform shape results may provide some insight into assumptions regarding FE model material property specifications. Assumptions that reduce the complexity of the models, and thus computational requirements, without sacrificing quality are important to identify. Posterior interface pressure waveforms at different locations during the same step tended to be of similar shape (though not necessarily of similar magnitude). Similarly, pressure-time waveforms in the lateral group (except at the LP site) tended to be similar in shape to each other. Anterior group RS-time plots, however, differed substantially from each other. The anterior surface has a relatively thin soft tissue layer over the bone, making local interface stress results highly sensitive to the geometrics, differences between the bone and the socket, and alignment of the bone relative to the socket, while the posterior and lateral regions have thicker soft tissue layers over bone, making local interface stress results less sensitive to these features. Thus,

FE model specifications on the anterior surface, particularly the geometries of the socket and bone, will likely need to be more accurately specified than those on the posterior and lateral surfaces.

Temporal Changes

Temporal interface stress changes are important because they affect the consistency of fit of the prosthesis. Consistent with previous findings (2,30), results here indicate that substantial changes in stresses occurred from one session to the next, provided sessions were more than a few days apart. Appoldt explains that for short leg-off times (on the order of a few minutes), no significant change in walking pressure was obtained as a specific function of the donning-doffing process (2). Our unpublished results from previous investigations suggest the same; sometimes the leg needed to be removed for short times to adjust the instrumentation, and we found no significant differences in steps before or after the interruption. In both studies, each subject used the same prosthesis with the same number of socks and same alignment in the different sessions for which the different stress magnitudes occurred. Thus, differences between sessions were not due to prosthesis modifications. Both investigators suggested residual limb volume changes were principal reasons for interface stress magnitude changes between sessions (2,30). Gait kinematics may also have changed.

It should be noted, however, that some investigators found substantial pressure changes from different trials conducted less than a few days apart (6), citing reproducibility as a problem in achieving consistent measurements, though it is not clear whether comparisons were from steps conducted minutes or hours apart. The researchers state that "the exact location of the stump in the socket varies slightly each time the limb is put on" and offer this as a principal reason for the lack of consistency. They also cite variations in gait, variations in the composition of the residual limb, and the type of suspension as sources of temporal variations. We expect that because these investigators taped transducers to the skin rather than mounting them to the socket wall, an important source of variability was instrumentation-related. The high sensitivity of measurements to positioning when no recession is made to accommodate the stiff transducer has been demonstrated and discussed above (31). We expect in the present study that residual limb geometry, material property changes, and possibly gait kinematics were the principal sources of the temporal changes for sessions conducted more than a few days apart.

Prosthetic socket design and alignment must accommodate differences in residual limb shape and material properties as well as changes in gait kinematics, a concept that is recognized clinically and is a feature that strongly contributes to the complexity of prosthetic design. Adding or removing socks and using flexible sockets are two means used clinically to try to reduce the detrimental effects of residual limb changes on socket comfort and fit. In the results presented here, these accommodations were not made, but instead, the same socket and same number of socks used in different sessions and the interface stress differences between sessions were compared. In both subjects, there was a mild trend of increased pressure coupled with decreased RS. This is a reasonable finding in that if a socket provided substantial pressure support, it would increase the total contact surface area and reduce the RS. This concept has been suggested in FE analysis conducted by Reynolds (21).

CONCLUSIONS

Principal conclusions from this study investigating interface pressures and shear stresses at 13 sites on two subjects with TTA are summarized below:

1. For both pressure and RS, anterior sites (distal or mid-limb) were the dominantly loaded of all sites tested. Lowest pressures and RSs were typically at LP sites.
2. AD pressures and RSs were consistently higher than those at AP, and the timings of maximal pressures at AD sites were significantly earlier than those at the AP sites in the same session.
3. LD pressures were typically higher than PF pressures. LP, LM, and LD RS maxima were typically of lower magnitude than those at the PF site.
4. In each session, mean time percentages into stance phase of pressure maxima for all posterior sites were within 11.6 percent of stance phase of each other.
5. Within a session, the sites of highest pressure and RS at the 1st pk were the same sites that experienced maximal pressures and RSs independent of stance phase time. Pressures and RSs at the 1st pk were within 10.6 percent of the maximal pressures and RSs independent of time except RS at the AMD site in one session (WP1024).

6. RSs at ALD, AMD, LD, and PD sites were directed more distally than proximally (i.e., $0^\circ < \text{RSang} < 180^\circ$). RS at LM, PF, and some LP sites were directed more proximally than distally (i.e., $180^\circ < \text{RSang} < 360^\circ$).
7. Differences in horizontal shear stress between ALD and AMD sites were always greater than zero, indicating skin tension across the tibial crest at AD locations. Differences in vertical shear stress between adjacent sites on the anterior surface were typically less than zero, reflecting in-plane compression in the skin in a proximal-distal direction; they were greater than zero in only a few selected cases.
8. Pressure-time curves were typically similar to each other in the posterior group, though their magnitudes were different. RS-time curves in the anterior group were typically not similar in shape to each other.
9. Differences in stress magnitudes between sessions conducted on the same subject (sessions more than 20 days apart) were apparent. In both subjects, there was a trend of increased pressure coupled with decreased RSs.

ACKNOWLEDGMENTS

Assistance in data collection, processing, and presentation by Russell Reed, David Berglund, Glenn Hwaung, and Santosh Zachariah is gratefully acknowledged.

REFERENCES

1. Appoldt FA, Bennett L. A preliminary report on dynamic socket pressures. Bull Prosthet Res 1967:10-8:20–55.
2. Appoldt FA, Bennett L, Contini R. Stump-socket pressure in lower extremity prostheses. J Biomech 1968:1:247–57.
3. Appoldt FA, Bennett L, Contini R. Tangential pressure measurement in above-knee suction sockets. Bull Prosthet Res 1970:10-13:70–86.
4. Leavitt LA, Peterson CR, Canzoneri J, Paz R, Muilenburg AL, Rhyne VT. Quantitative method to measure the relationship between prosthetic gait and the forces produced at the stump-socket interface. Am J Phys Med 1970:49(3):192–203.
5. Sonck WA, Cockrell JL, Koepke GH. Effect of liner materials on interface pressures in below-knee prostheses. Arch Phys Med Rehabil 1970:51:666–9.
6. Rae JW, Cockrell JL. Interface pressure and stress distribution in prosthetic fitting. Bull Prosthet Res 1971:10-15:64–111.
7. Leavitt LA, Zuniga EN, Calvert JC, Canzoneri J, Peterson CR. Gait analysis and tissue-socket interface pressures in above-knee amputees. Southern Med J 1972:65(10):1197–207.
8. Pearson JR, Holmgren G, March L, Öberg K. Pressures in critical regions of the below-knee patellar-tendon-bearing prosthesis. Bull Prosthet Res 1973:10-19:52–76.
9. Pearson JR, Grevsten S, Almby B, Marsh L. Pressure variation in the below-knee patellar tendon bearing suction socket prosthesis. J Biomech 1974:7:487–96.
10. Bielefeldt A, Schreck HJ. The altered alignment influence on above-knee prosthesis socket pressure distribution. Int Ser Biomech 1979:3(A):387–93.
11. Winarski DJ, Pearson JR. Least-squares matrix correlations between stump stresses and prosthesis loads for below-knee amputees. J Biomech Eng 1987:109:238–46.
12. Sanders JE, Daly CH, Burgess EM. Interface shear stresses during ambulation with a below-knee prosthetic limb. J Rehabil Res Dev 1992:29(4):1–8.
13. Williams RB, Porter D, Roberts VC, Regan JF. Triaxial force transducer for investigating stresses at the stump/socket interface. Med Biol Eng Comput 1992:30:89–96.
14. Engsberg JR, Springer MJ, Harder JA. Quantifying interface pressures in below-knee amputee sockets. J Assoc Child Prosthet Orthot Clin 1992:27(3):81–8.
15. Sanders JE, Daly CH, Burgess EM. Clinical measurement of normal and shear stresses on a transtibial residual limb: characteristics of waveform shapes during walking. Prosthet Orthot Int 1993:17(1):38–48.
16. Steege JW, Childress DS. Finite element prediction of pressure at the below-knee socket interface. In: Report of ISPO Workshop on CAD/CAM in Prosthetics and Orthotics, Seattle, WA, 1988:71–82.
17. Silver-Thorn MB. Prediction and experimental verification of residual limb/prosthetic socket interface pressures for below-knee amputees (Dissertation). Evanston, IL: Northwestern University, 1991.
18. Brennan JM, Childress DS. Finite element and experimental investigation of above-knee amputee limb/prosthesis systems: a comparative study. Adv Bioeng, ASME WAM, 1991:BED-20:547–50.
19. Sanders JE, Daly CH. Normal and shear stresses on a residual limb in a prosthetic socket during ambulation: comparison of finite element results with experimental measurements. J Rehabil Res Dev 1993:30(2):191–204.
20. Quesada P, Skinner HB. Analysis of a below-knee patellar tendon-bearing prosthesis: a finite element study. J Rehabil Res Dev 1991:28(3):1–12.
21. Reynolds DP, Lord M. Interface load analysis for computer-aided design of below-knee prosthetic sockets. Med Biol Eng Comput 1992:30:419–26.
22. Zhang M, Lord M, Turner-Smith AR, Roberts VC. Development of a non-linear finite element modelling of the below-knee prosthetic socket interface. Med Eng Phys 1995:17(8):559–66.
23. Steege JW, Childress DS. Analysis of trans-tibial prosthetic gait using the finite element technique. In: Proceedings of the 21st Annual Meeting and Scientific Symposium AAOP, New Orleans, 1995:13–4.
24. Radcliffe CW, Foort J. The patellar-tendon-bearing below-knee prosthesis. Biomechanics Laboratory, University of California, Berkeley, 1961.

25. Sanders JE, Daly CH. Measurement of stresses in three orthogonal directions at the residual limb/prosthetic socket interface. IEEE Trans Rehabil Eng 1993:1(2):79–85.
26. Sanders JE, Smith LM, Spelman FA. A small and lightweight three-channel signal-conditioning unit for strain-gage transducers. J Rehabil Res Dev 1995:32(3):210–3.
27. Appoldt FA, Bennett L, Contini R. Socket pressure as a function of pressure transducer protrusion. Bull Prosthet Res 1969:10-11:236–49.
28. Sanders JE, Daly CH, Cummings WR, Reed RD, Marks RJ II. A measurement device to assist amputee prosthetic fitting. J Clin Eng 1994:19(1):63–71.
29. Technical Committee 168, International Organization for Standardization (ISO). Prosthetics: structural testing of lower limb prostheses, 1994.
30. Sanders JE. Ambulation with a prosthetic limb: mechanical stresses in amputated limb tissues (Dissertation). Seattle, WA: University of Washington, 1991.
31. Patterson RP, Fisher SV. The accuracy of electrical transducers for the measurement of pressure applied to the skin. IEEE Trans Biomed Eng 1979:26:450–6.
32. Bennett L, Kavner D, Lee BK, Trainor FA. Shear vs pressure as causative factors in skin blood flow occlusion. Arch Phys Med Rehabil 1979:60:309–14.
33. Burgess EM, Moore AJ. A study of interface pressures in the below-knee prosthesis (physiological suspension: an interim report). Bull Prosthet Res, Fall 1977:10-28:58–70.
34. Vannah WM. Indentor tests and finite element modelling of bulk muscular tissue in vivo (Dissertation). Evanston, IL: Northwestern University, 1990
35. Lanir Y, Fung YC. Two-dimensional mechanical properties of rabbit skin: II. experimental results. J Biomech 1974:7:171–82.